Measurements of Field Quality in Helical Dipoles for RHIC

A. Jain, G. Ganetis, W. Louie, A. Marone,
J. Muratore, R. Thomas, P. Wanderer and E. Willen

Superconducting Magnet Division
Brookhaven National Laboratory
Upton, New York 11973-5000, USA

Introduction

- BNL is producing helical dipoles for Siberian Snakes and Spin Rotators to be installed in RHIC under a joint BNL-RIKEN spin physics program.
- The dipole field in these magnets rotates by 360 degrees over a length of 2.4 meters. This feature makes the measurements of these magnets more difficult than usual accelerator magnets with essentially a 2-D field over most of the length.

Picture of a helical dipole coil

Axial Variation of Dipole Field Components

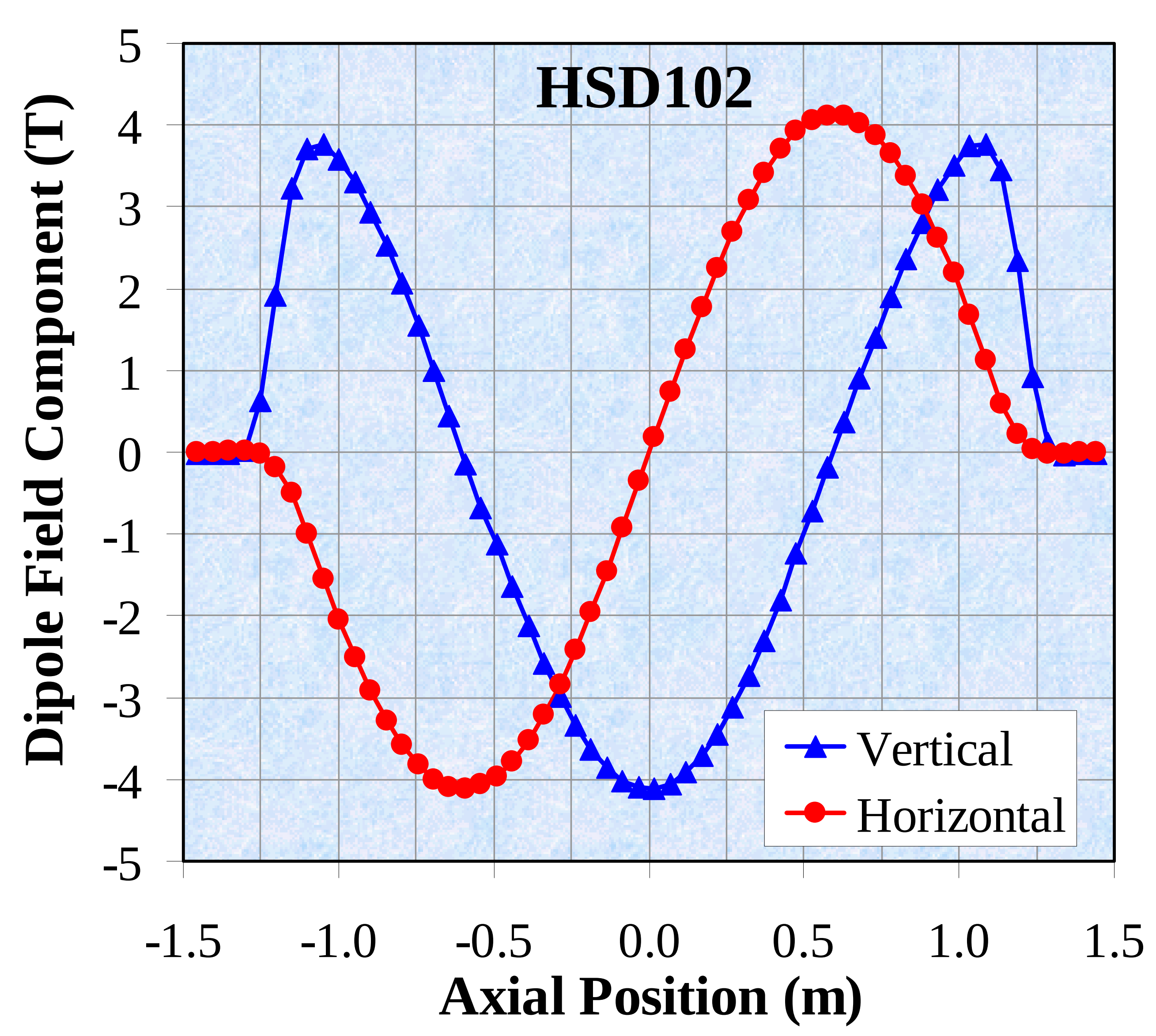

Harmonic Expansion

- Axial variation results in a 3-D field.
- A simple harmonic expansion results under the assumption of periodicity along the *Z*-axis with wavelength λ:

$$B_{r,\theta,z}(r,\theta,z) \equiv B_{r,\theta,z}(r,\tilde{\theta}); \quad \tilde{\theta} = \theta - kz$$

$$k = (d\alpha / dz) = \text{rate of change of dipole field angle} = 2\pi / \lambda$$

$$B_r(r,\tilde{\theta}) = B_0 \sum_{n=1}^{\infty} \left[\frac{2^n n!}{n^n (kR_{ref})^{n-1}} \right] I_n'(nkr) \left[\tilde{b}_n \sin(n\tilde{\theta}) + \tilde{a}_n \cos(n\tilde{\theta}) \right]$$

$$B_\theta(r,\tilde{\theta}) = B_0 \sum_{n=1}^{\infty} \left[\frac{2^n n!}{n^n (kR_{ref})^{n-1}} \right] \frac{I_n(nkr)}{kr} \left[\tilde{b}_n \cos(n\tilde{\theta}) - \tilde{a}_n \sin(n\tilde{\theta}) \right]$$

$$B_z(r,\tilde{\theta}) = -(kr) B_\theta(r,\tilde{\theta})$$

$n = 1$ is Dipole term, etc.

Harmonic Expansion

- $\tilde{b}_n$ and $\tilde{a}_n$ are ideally constants, representing the normal and the skew components in a reference frame that rotates along the magnet length.
- In a reference frame fixed in space, the normal and the skew coefficients are functions of the axial position:

$$b_n(z) = \tilde{b}_n \cos(nkz) + \tilde{a}_n \sin(nkz)$$

$$a_n(z) = \tilde{a}_n \cos(nkz) - \tilde{b}_n \sin(nkz)$$

- All harmonics oscillate with axial position; the higher harmonics do so more rapidly.
- This implies that if a conventional rotating coil is employed to measure the harmonics, the coil must be as short as possible to avoid cancellation of signal over its length.

Measuring Coil Parameters

- 34.2 mm radius (Reference radius for these magnets is 31 mm)
- Only 51 mm long, less than one diameter, and about 2% of the wavelength.
- Tangential winding: 56 turns, 15.4 degrees.
- Two Dipole Buck windings: 6 turns each.
- The no. of turns is about twice the typical RHIC coils, to compensate for lower signal due to the short length.
- Has two quadrupole buck windings also, but these are not used for the dipole tests.

Flux through a Tangential Coil

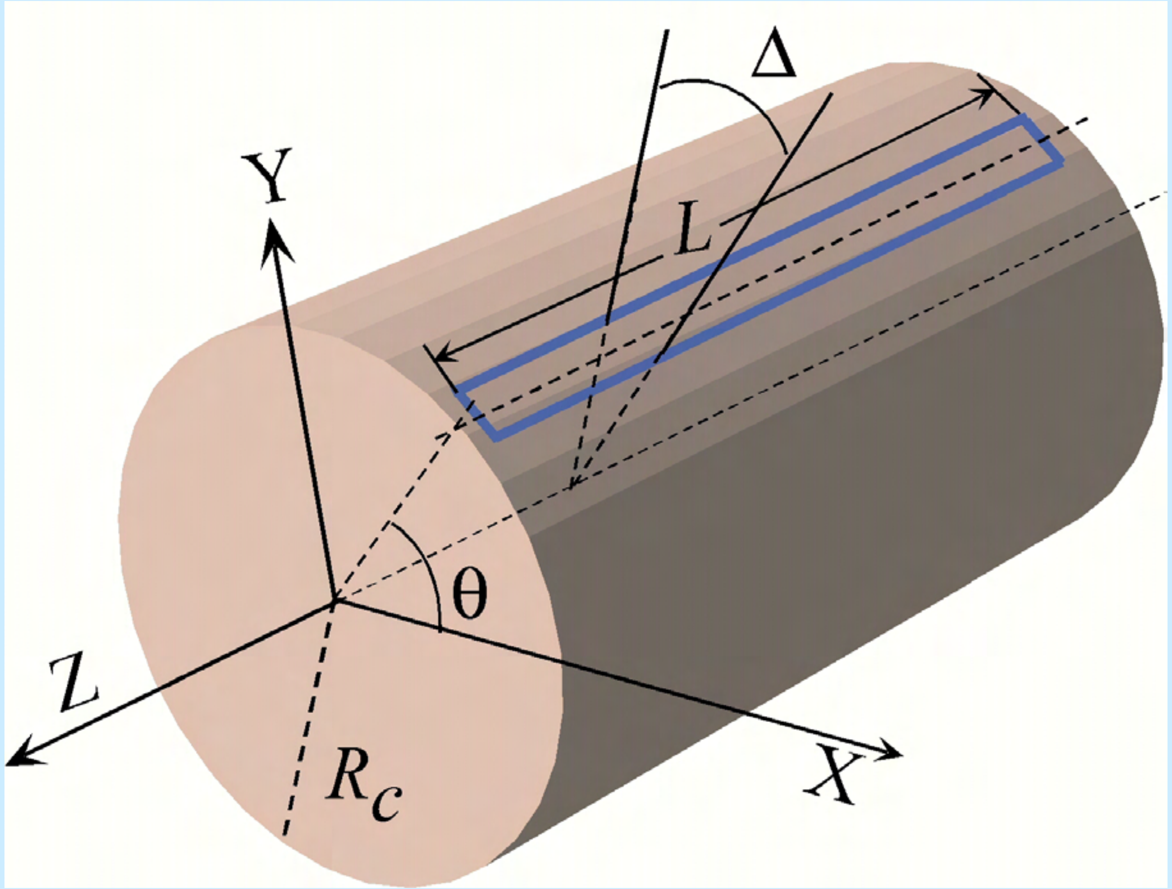

$$\Phi(\theta, z) = N \int_{\theta-\Delta/2}^{\theta+\Delta/2} \int_{z-L/2}^{z+L/2} B_r(R_c, \theta, z) \cdot R_c \; dz \, d\theta$$

Flux through a Tangential Coil

$$\Phi(\theta, z) = \sum_{n=1}^{\infty} \Re_n(R_c)\left[\frac{2NLR_c}{n}\right]\sin\left(\frac{n\Delta}{2}\right)$$

$$\times\left[\frac{\sin(nkL/2)}{nkL/2}\right]$$

$$\times\left[A_n(z)\cos(n\theta) + B_n(z)\sin(n\theta)\right]$$

where $\tilde{A}_n$ and $\tilde{B}_n$ are assumed constants over the coil length, and

$$\Re_n(r) = \left[\frac{2^n n!}{n^n (kR_{ref})^{n-1}}\right] I_n'(nkr)$$

$\Re_n(r)$ differs from $\left(r/R_{ref}\right)^{n-1}$ by 0.25% for the dipole term and by 2.7% for the 30 - pole term for $r = R_{ref} = 31$ mm.

The voltage signals can be computed from the above expression for the flux. These expressions are used to analyze the data.

Results

- Measurements as a function of current at a single location in the center of the magnet .
  [*Gives saturation behaviour of various harmonics*.]
- Measurements as a function of axial position at several currents (Z-scans, typically at 102 A, 267 A and 329 A)
  [*Gives uniformity of field quality over the magnet length*, *as well as harmonics in the ends*.]

It should be noted that the data analysis requires knowledge of the twist pitch, *k*. The design value of 2.618 m^{-1} corresponding to λ = 2.4 m is used. The analysis is not strictly valid in the ends, but the error is expected to be only a few percent for the harmonics of interest, and is neglected.

Variation of harmonics with current

- There is considerable magnet to magnet variation in the geometric harmonics. This makes it difficult to compare the saturation behaviour of different magnets in a plot of raw data.
- There are several types of dipoles – with left handed and right handed rotations, and with the dipole field either vertical or horizontal at the center position.
- To compare all the magnets in a single plot, the harmonics are expressed in a coordinate system where the Y-axis coincides with the dipole field
- Two plots for each harmonic are presented here. An “unshifted” plot shows the raw data, indicating the range of geometric values. A “shifted” plot shows the same data after the value at 102 A (up ramp) is subtracted out to eliminate geometric differences between different magnets.

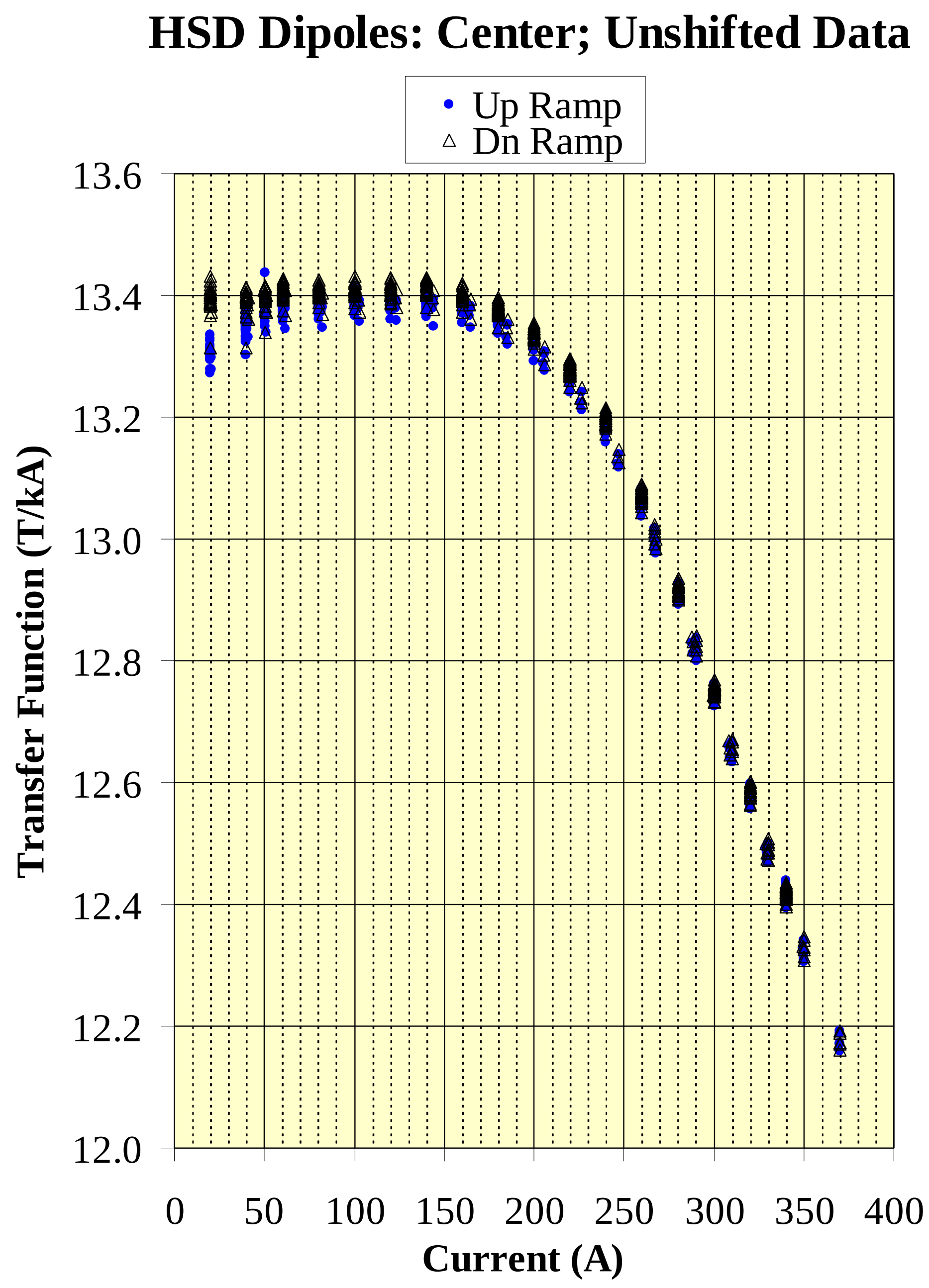
HSD Dipoles: Center; Unshifted Data
Up Ramp
Dn Ramp
Transfer Function (T/kA)
Current (A)
13.6
13.4
13.2
13.0
12.8
12.6
12.4
12.2
12.0
0
50
100
150
200
250
300
350
400

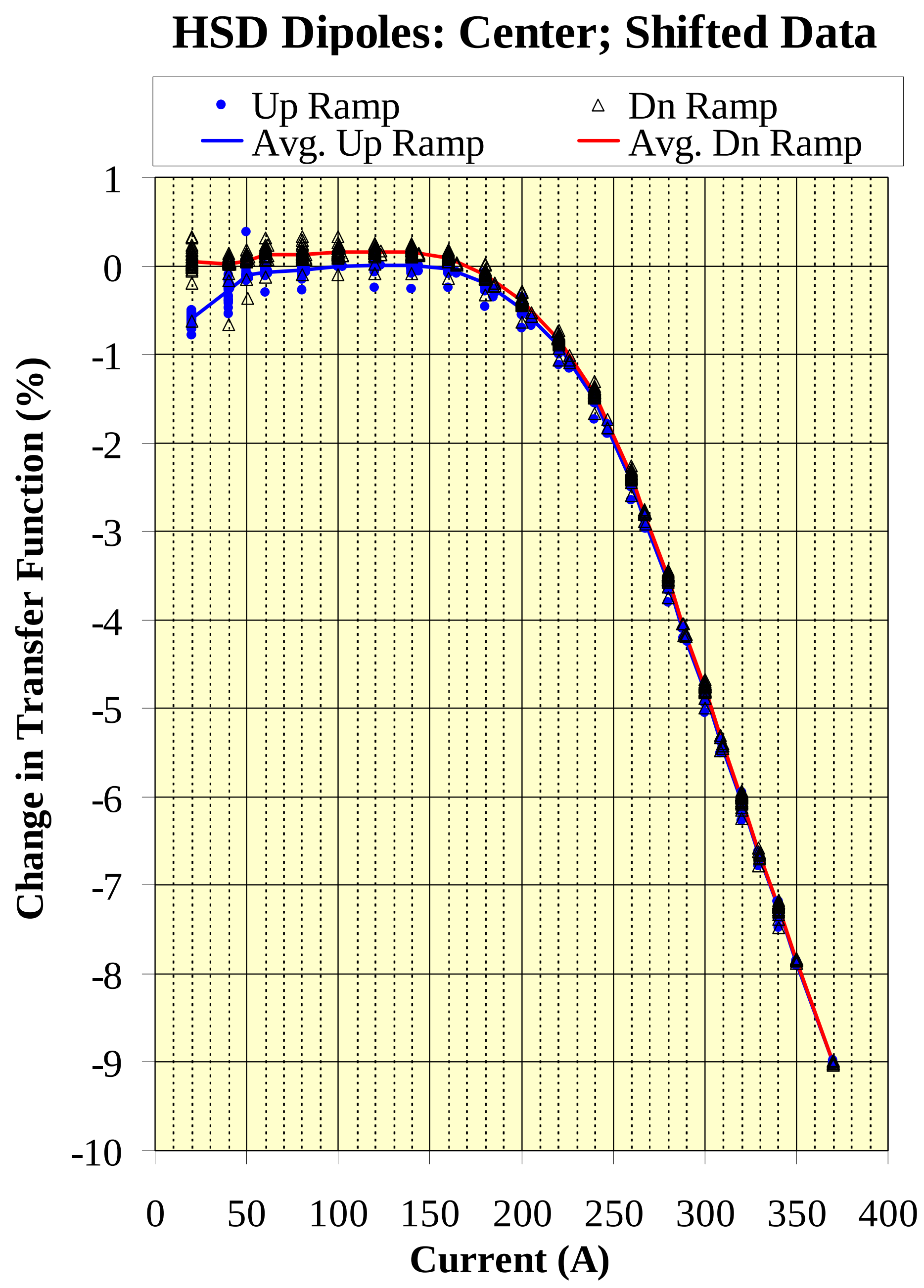
HSD Dipoles: Center; Shifted Data
Up Ramp
Dn Ramp
Avg. Up Ramp
Avg. Dn Ramp
Change in Transfer Function (%)
Current (A)
1
0
-1
-2
-3
-4
-5
-6
-7
-8
-9
-10
0
50
100
150
200
250
300
350
400

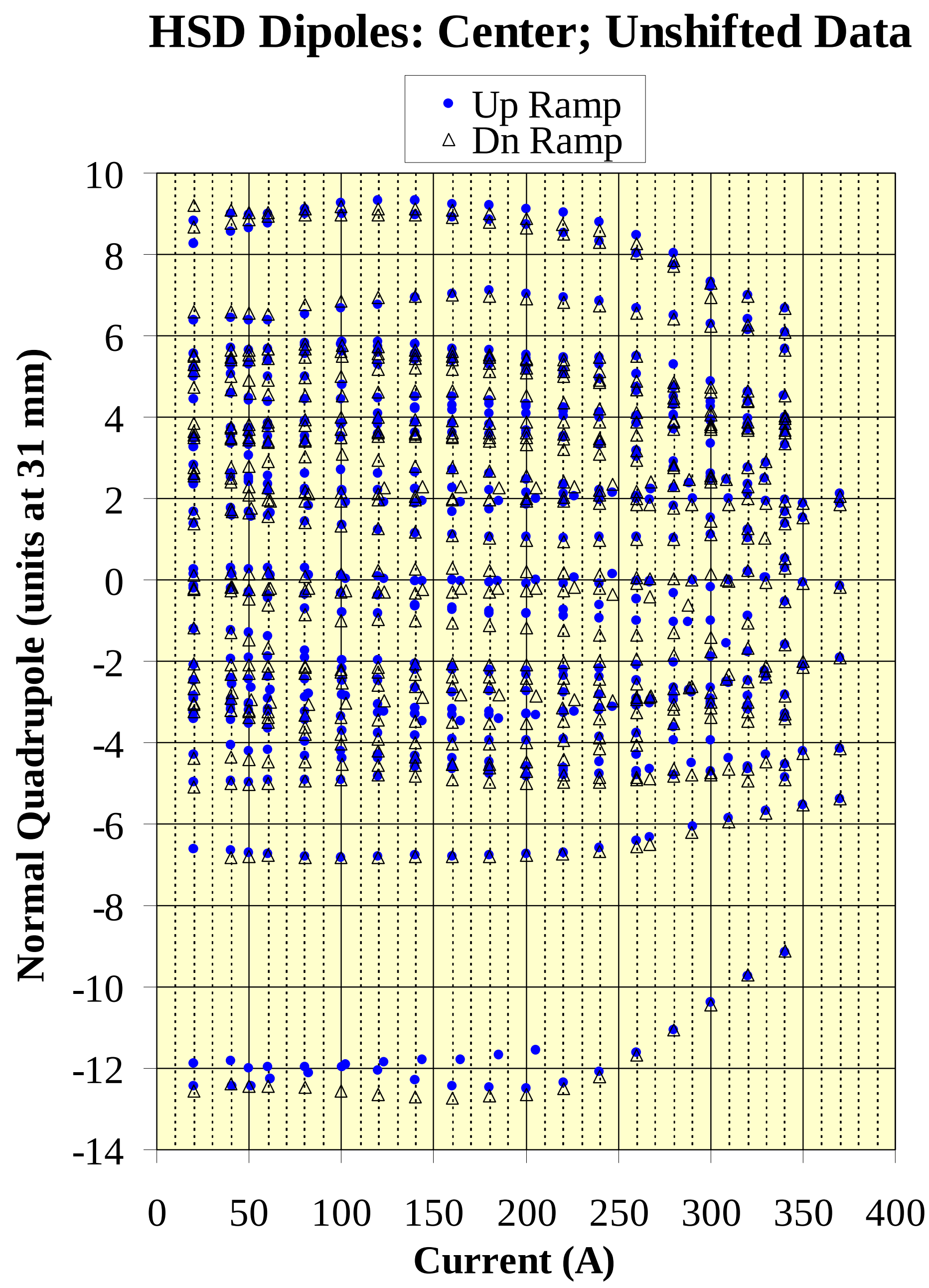
HSD Dipoles: Center; Unshifted Data
Up Ramp
Dn Ramp
Normal Quadrupole (units at 31 mm)
Current (A)
10
8
6
4
2
0
-2
-4
-6
-8
-10
-12
-14
0
50
100
150
200
250
300
350
400

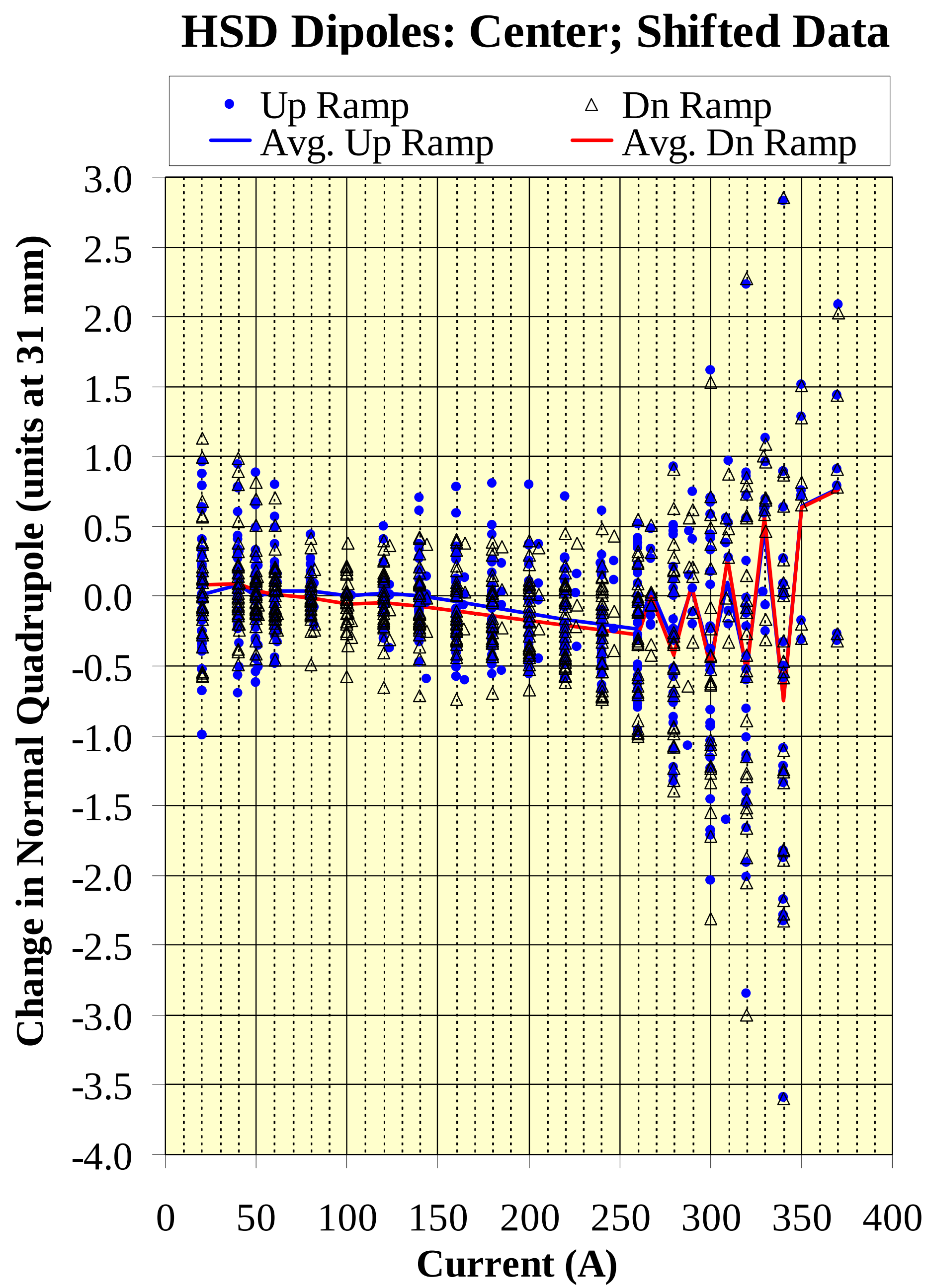
HSD Dipoles: Center; Shifted Data
Up Ramp
Dn Ramp
Avg. Up Ramp
Avg. Dn Ramp
Change in Normal Quadrupole (units at 31 mm)
Current (A)
3.0
2.5
2.0
1.5
1.0
0.5
0.0
-0.5
-1.0
-1.5
-2.0
-2.5
-3.0
-3.5
-4.0
0
50
100
150
200
250
300
350
400

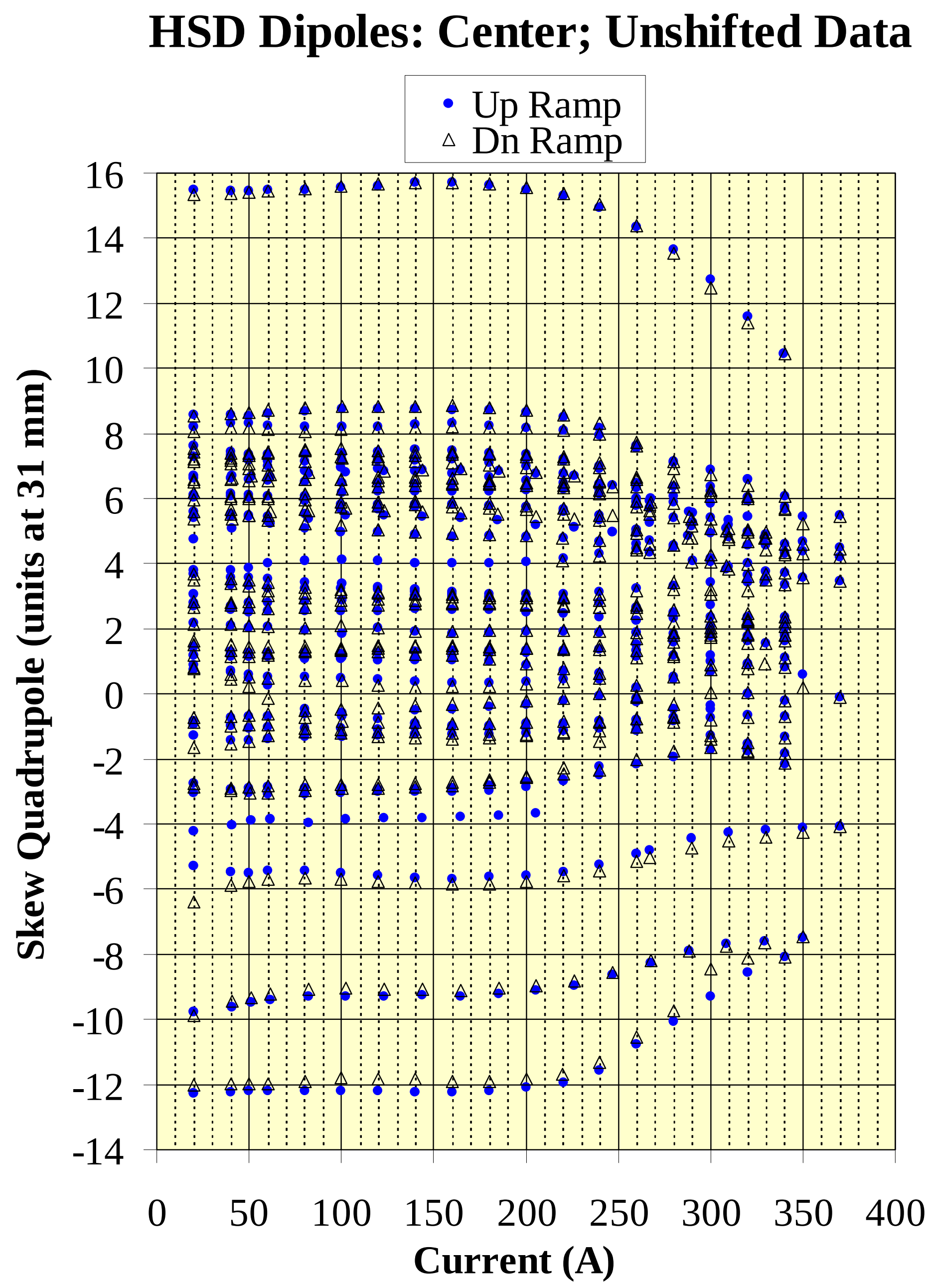
HSD Dipoles: Center; Unshifted Data
Up Ramp
Dn Ramp
Skew Quadrupole (units at 31 mm)
Current (A)
16
14
12
10
8
6
4
2
0
-2
-4
-6
-8
-10
-12
-14
0
50
100
150
200
250
300
350
400

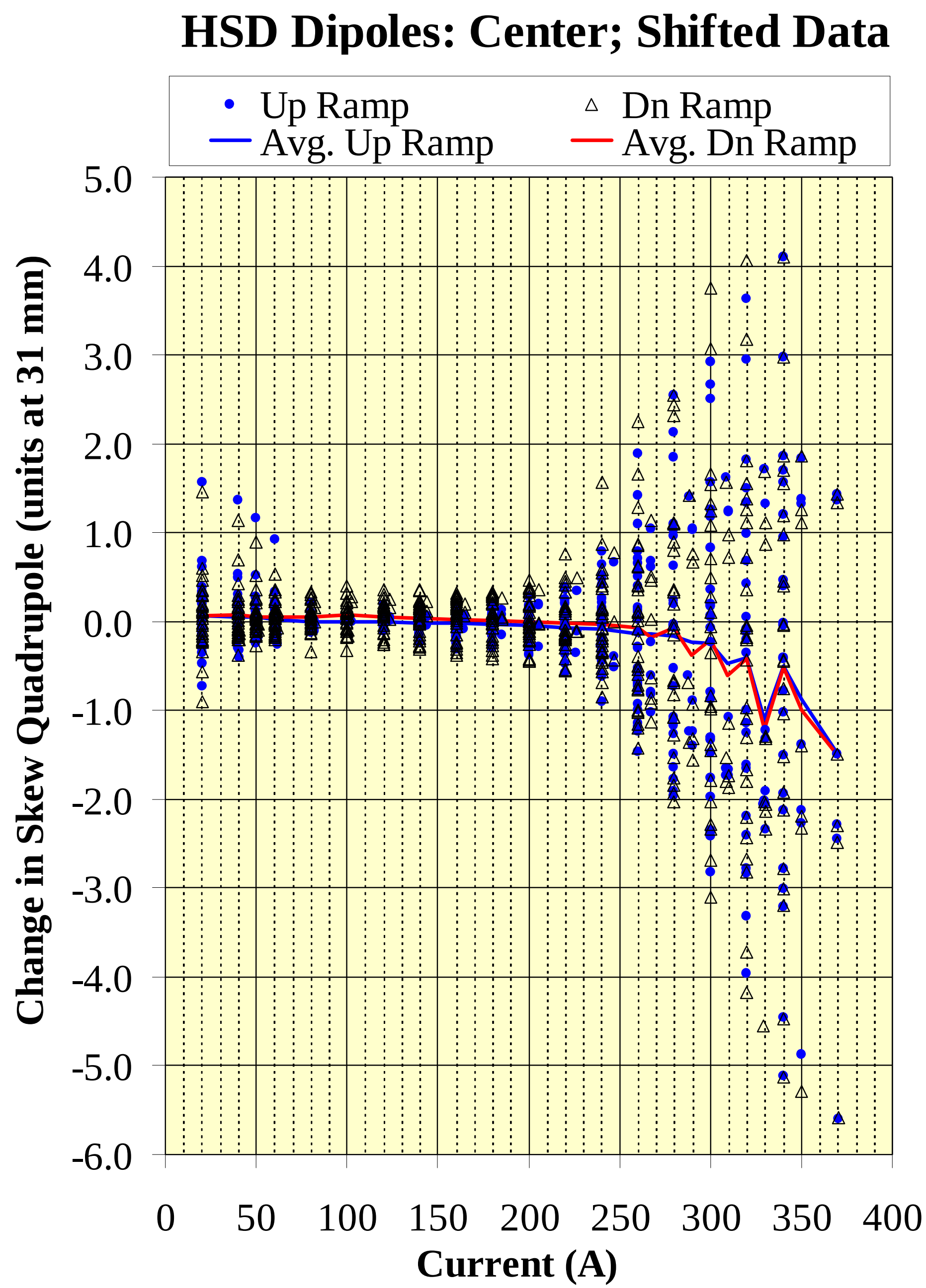
HSD Dipoles: Center; Shifted Data
Up Ramp
Dn Ramp
Avg. Up Ramp
Avg. Dn Ramp
Change in Skew Quadrupole (units at 31 mm)
Current (A)
5.0
4.0
3.0
2.0
1.0
0.0
-1.0
-2.0
-3.0
-4.0
-5.0
-6.0
0
50
100
150
200
250
300
350
400

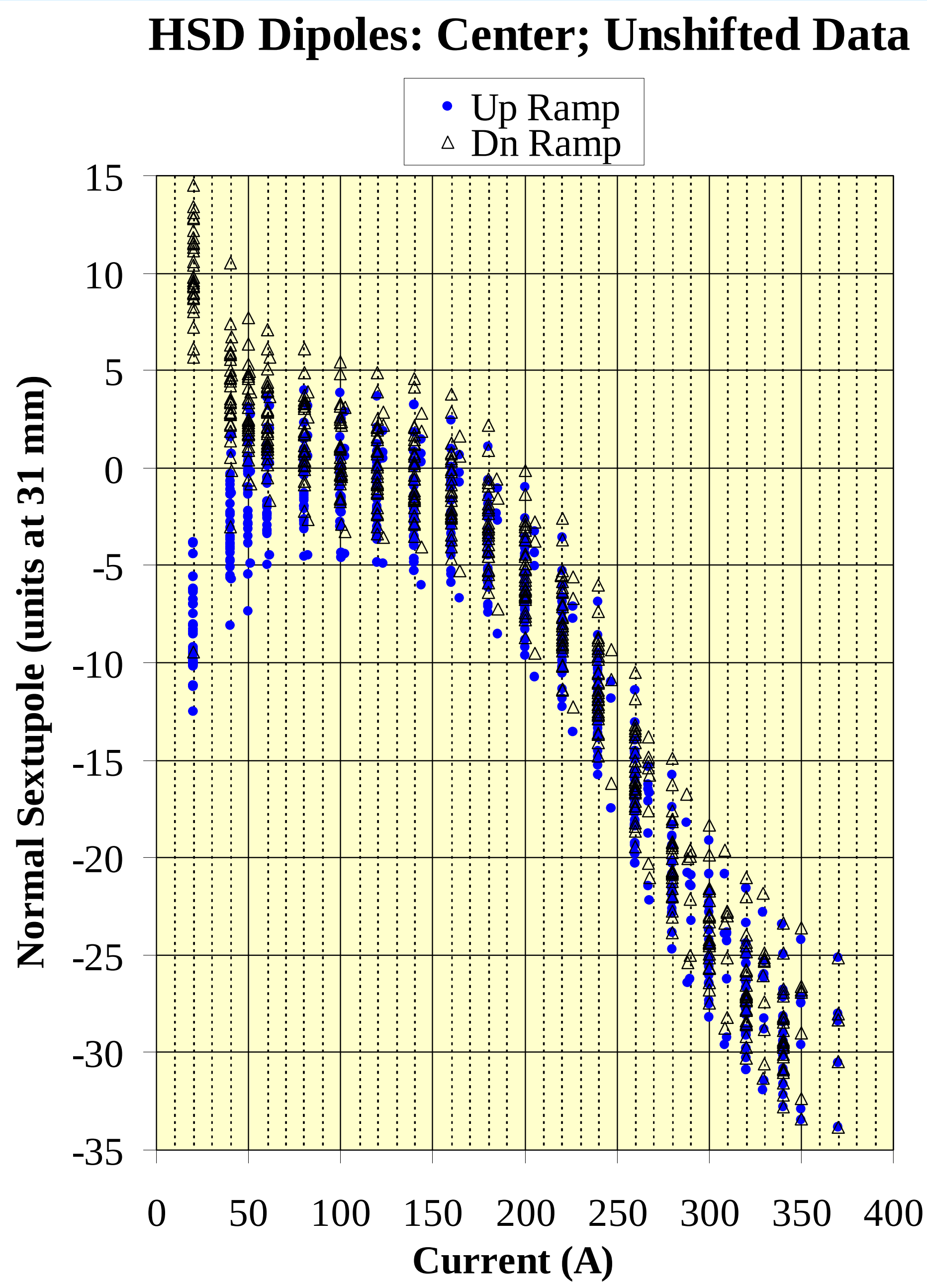
HSD Dipoles: Center; Unshifted Data
Up Ramp
Dn Ramp
Normal Sextupole (units at 31 mm)
15
10
5
0
-5
-10
-15
-20
-25
-30
-35
0
50
100
150
200
250
300
350
400
Current (A)

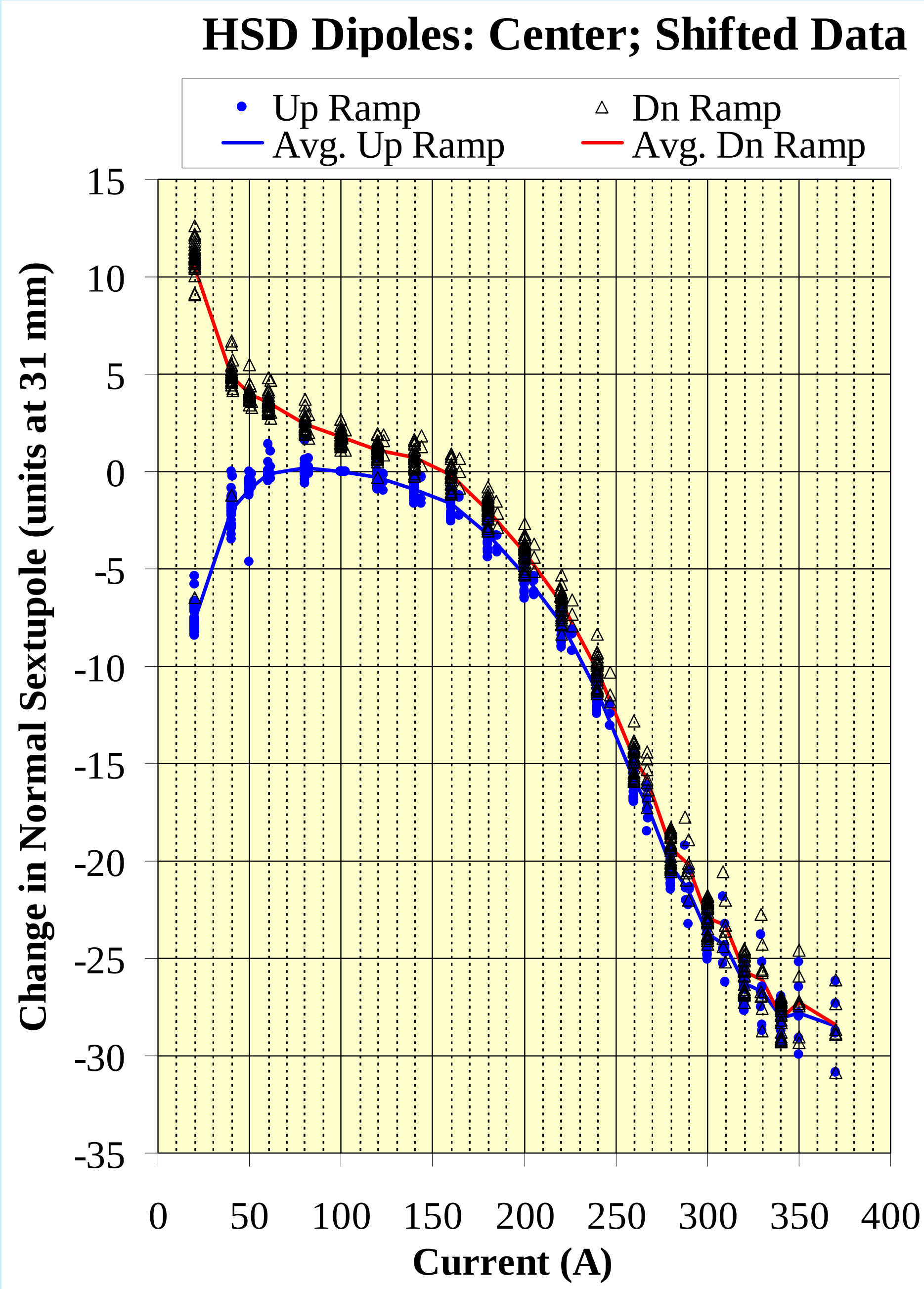
HSD Dipoles: Center; Shifted Data
Up Ramp
Dn Ramp
Avg. Up Ramp
Avg. Dn Ramp
Change in Normal Sextupole (units at 31 mm)
15
10
5
0
-5
-10
-15
-20
-25
-30
-35
0
50
100
150
200
250
300
350
400
Current (A)

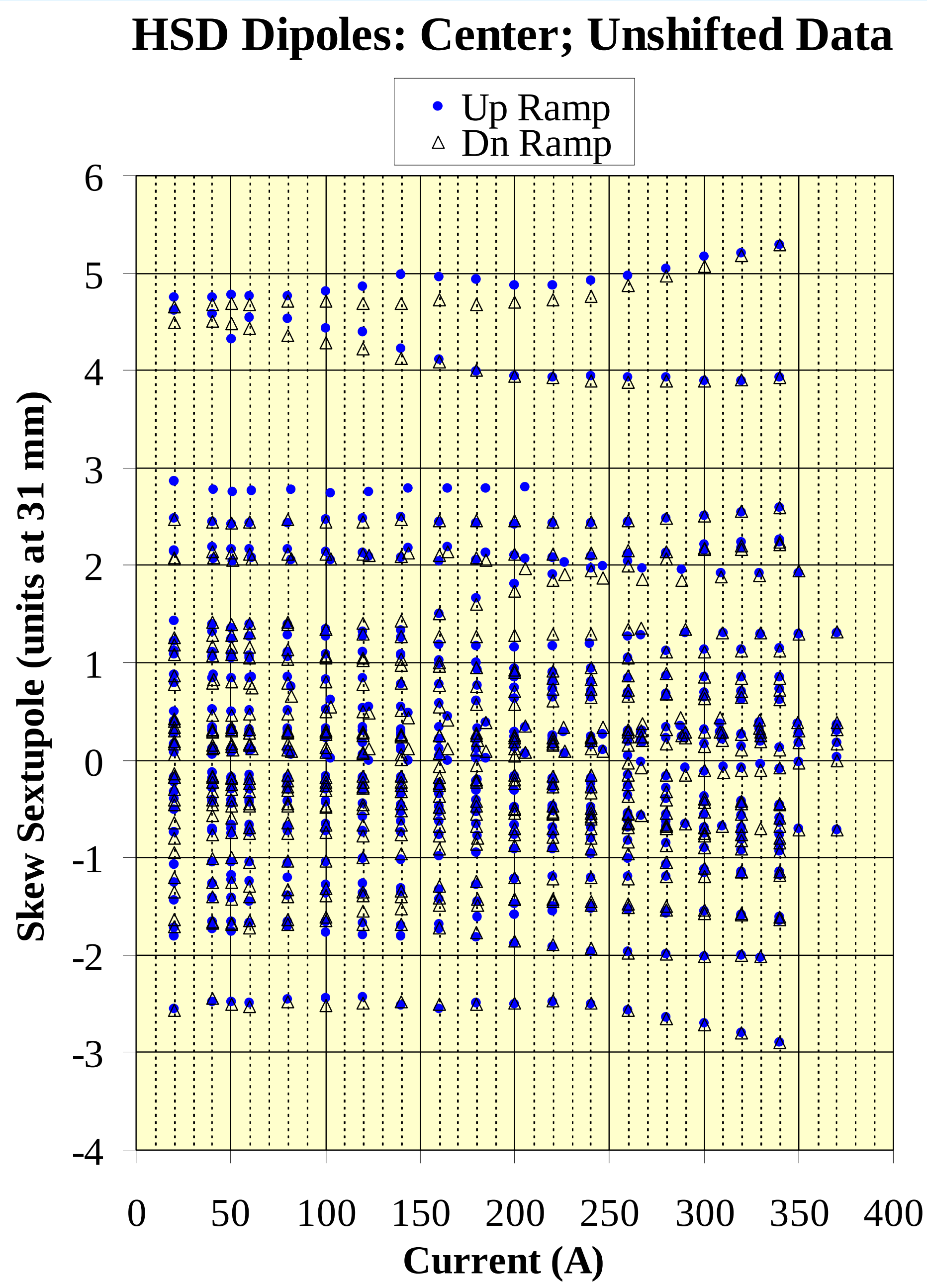
HSD Dipoles: Center; Unshifted Data
Up Ramp
Dn Ramp
Skew Sextupole (units at 31 mm)
Current (A)
6
5
4
3
2
1
0
-1
-2
-3
-4
0
50
100
150
200
250
300
350
400

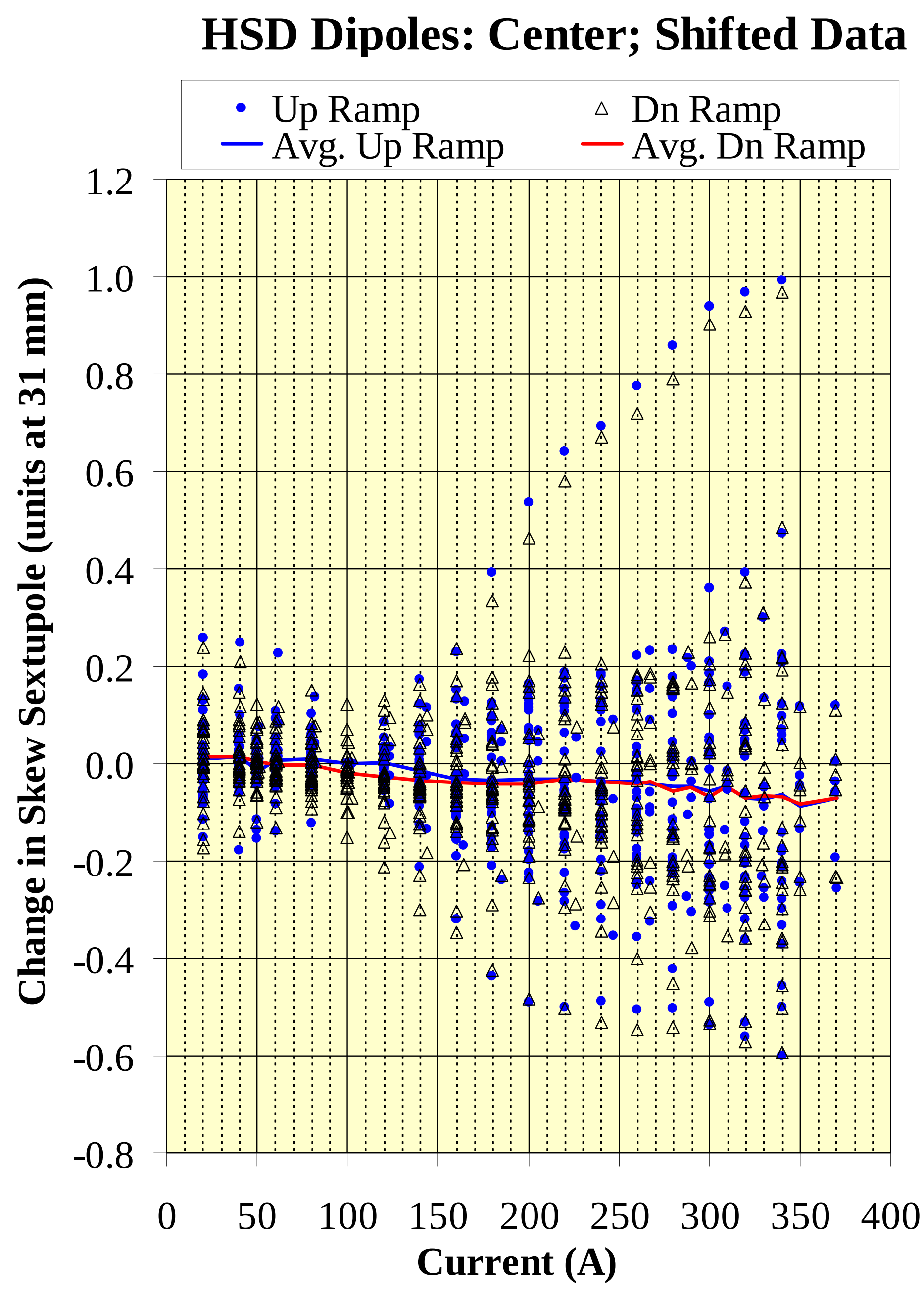
HSD Dipoles: Center; Shifted Data
Up Ramp
Dn Ramp
Avg. Up Ramp
Avg. Dn Ramp
Change in Skew Sextupole (units at 31 mm)
Current (A)
1.2
1.0
0.8
0.6
0.4
0.2
0.0
-0.2
-0.4
-0.6
-0.8
0
50
100
150
200
250
300
350
400

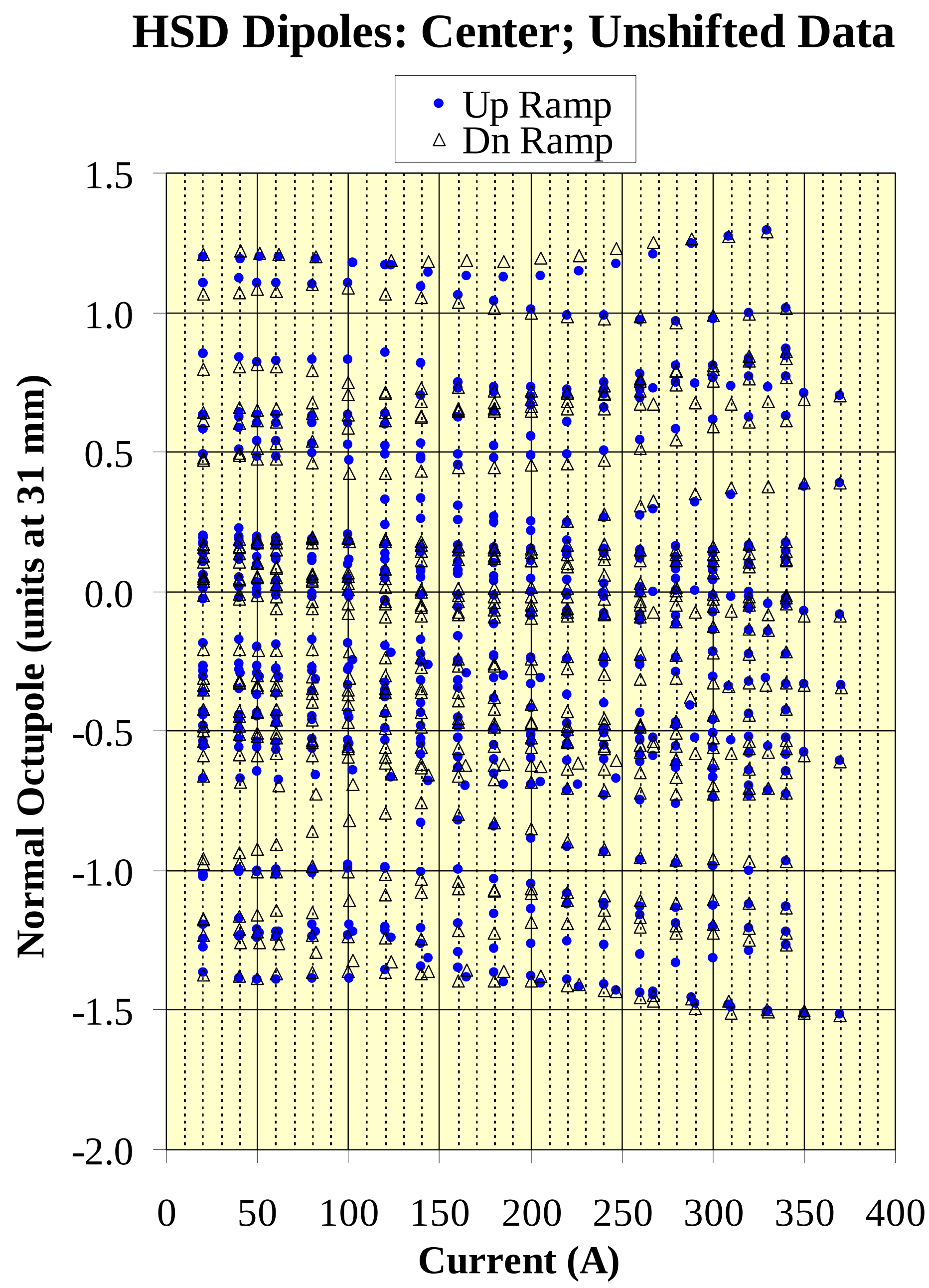
HSD Dipoles: Center; Unshifted Data
Up Ramp
Dn Ramp
1.5
1.0
0.5
0.0
-0.5
-1.0
-1.5
-2.0
Normal Octupole (units at 31 mm)
0
50
100
150
200
250
300
350
400
Current (A)

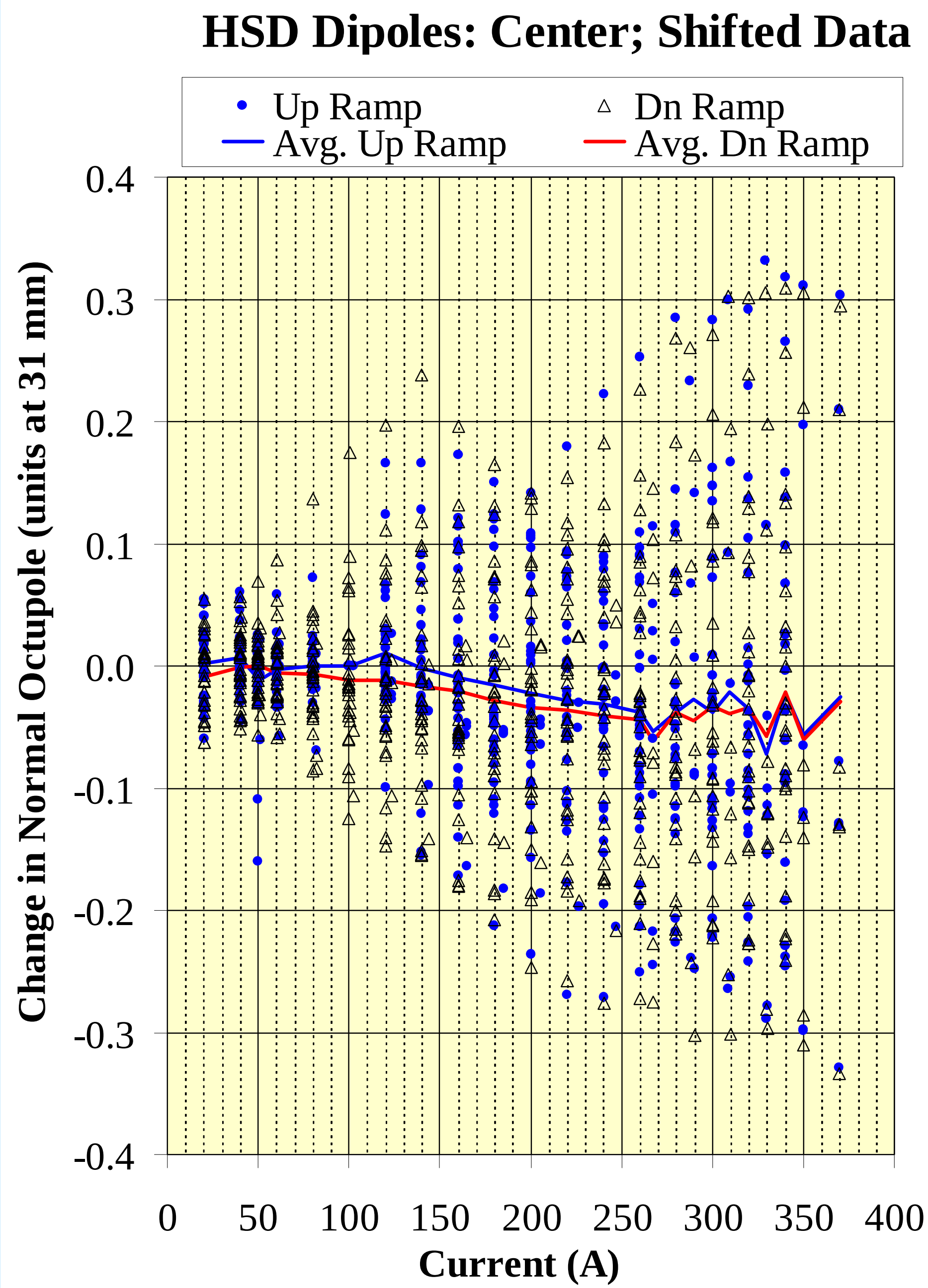
HSD Dipoles: Center; Shifted Data
Up Ramp
Dn Ramp
Avg. Up Ramp
Avg. Dn Ramp
0.4
0.3
0.2
0.1
0.0
-0.1
-0.2
-0.3
-0.4
Change in Normal Octupole (units at 31 mm)
0
50
100
150
200
250
300
350
400
Current (A)

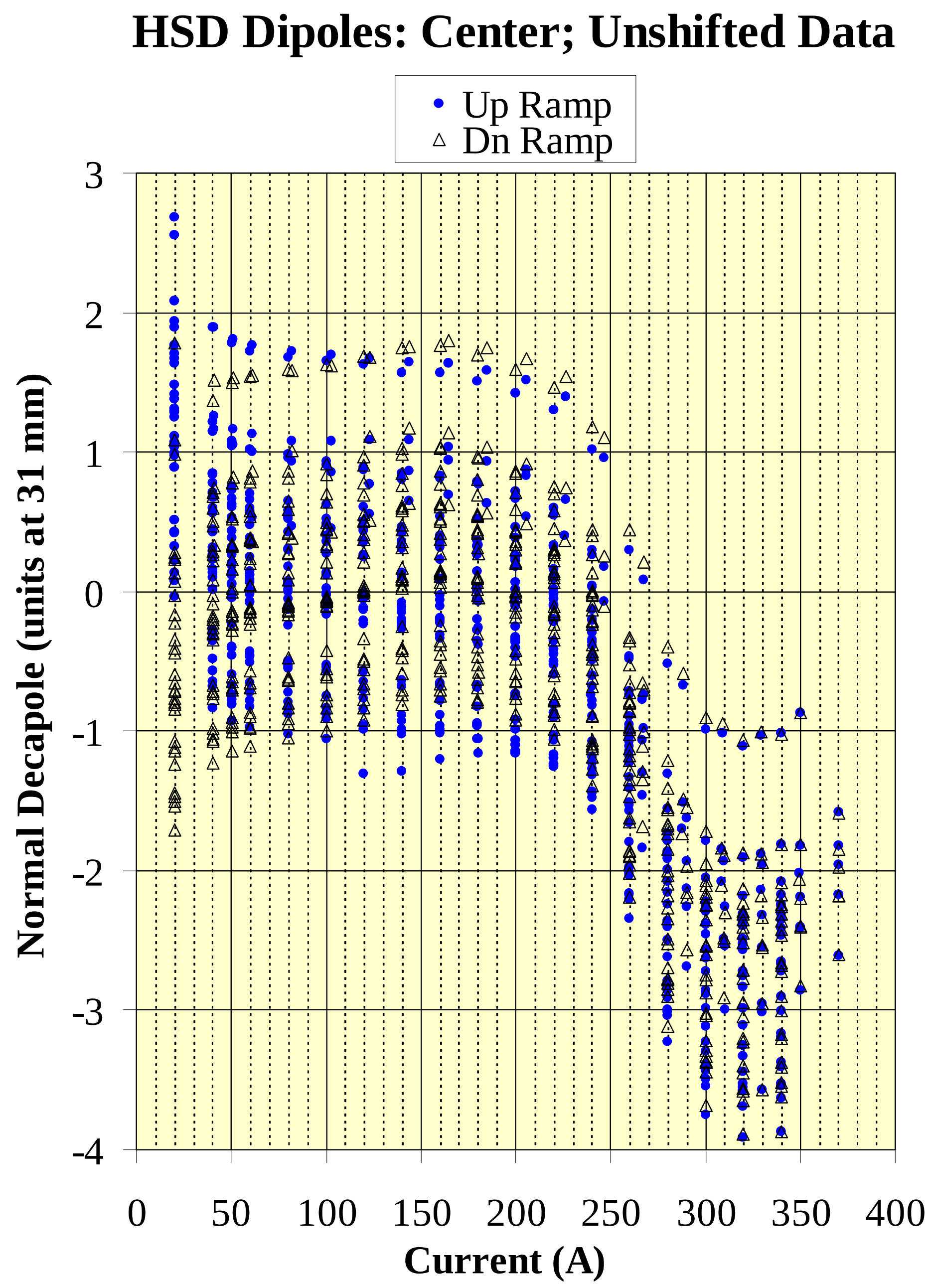
HSD Dipoles: Center; Unshifted Data
Up Ramp
Dn Ramp
Normal Decapole (units at 31 mm)
Current (A)
3
2
1
0
-1
-2
-3
-4
0
50
100
150
200
250
300
350
400

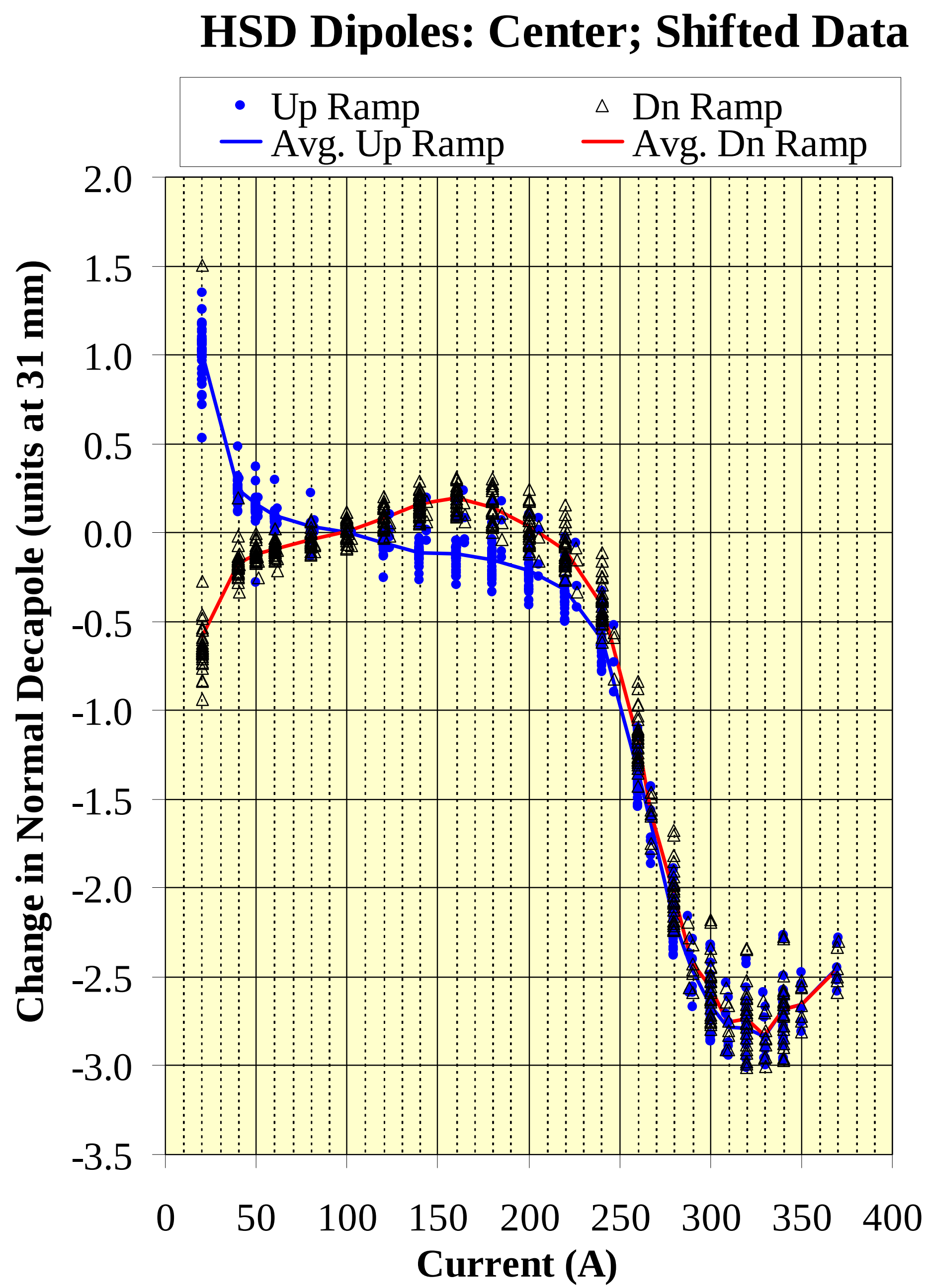
HSD Dipoles: Center; Shifted Data
Up Ramp
Dn Ramp
Avg. Up Ramp
Avg. Dn Ramp
Change in Normal Decapole (units at 31 mm)
Current (A)
2.0
1.5
1.0
0.5
0.0
-0.5
-1.0
-1.5
-2.0
-2.5
-3.0
-3.5
0
50
100
150
200
250
300
350
400

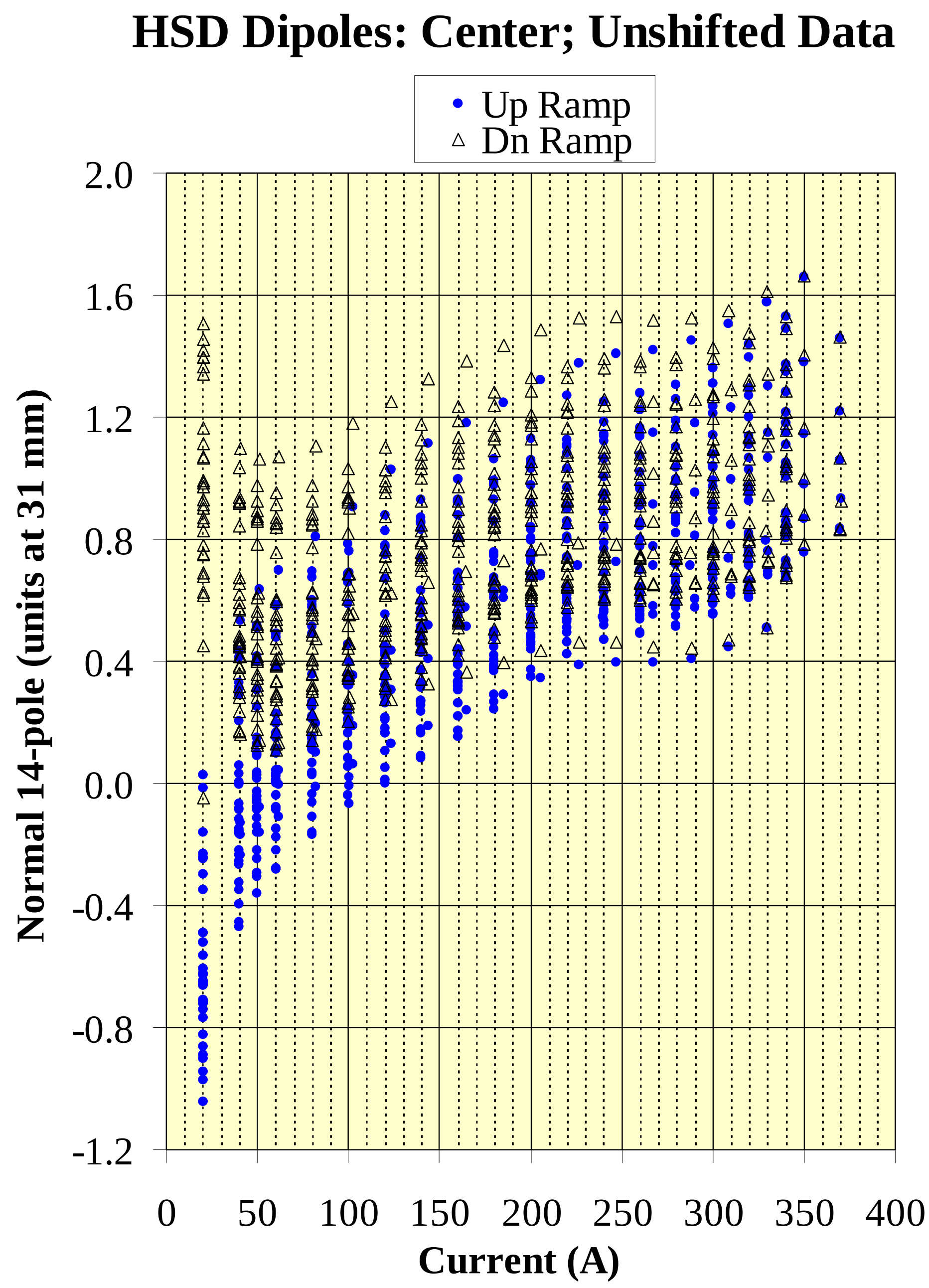
HSD Dipoles: Center; Unshifted Data
Up Ramp
Dn Ramp
2.0
1.6
1.2
0.8
0.4
0.0
-0.4
-0.8
-1.2
0
50
100
150
200
250
300
350
400
Current (A)
Normal 14-pole (units at 31 mm)

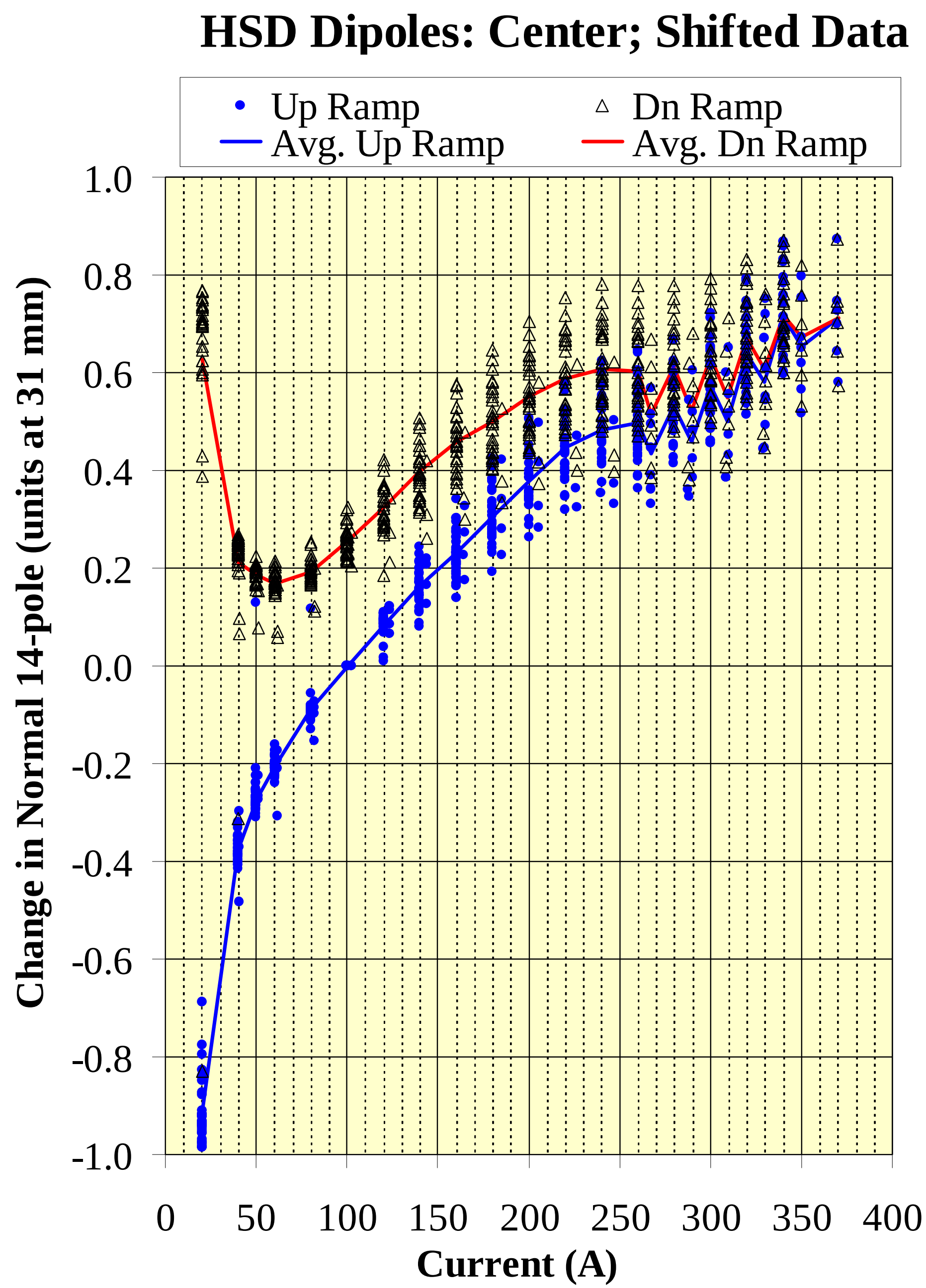
HSD Dipoles: Center; Shifted Data
Up Ramp
Dn Ramp
Avg. Up Ramp
Avg. Dn Ramp
1.0
0.8
0.6
0.4
0.2
0.0
-0.2
-0.4
-0.6
-0.8
-1.0
0
50
100
150
200
250
300
350
400
Current (A)
Change in Normal 14-pole (units at 31 mm)

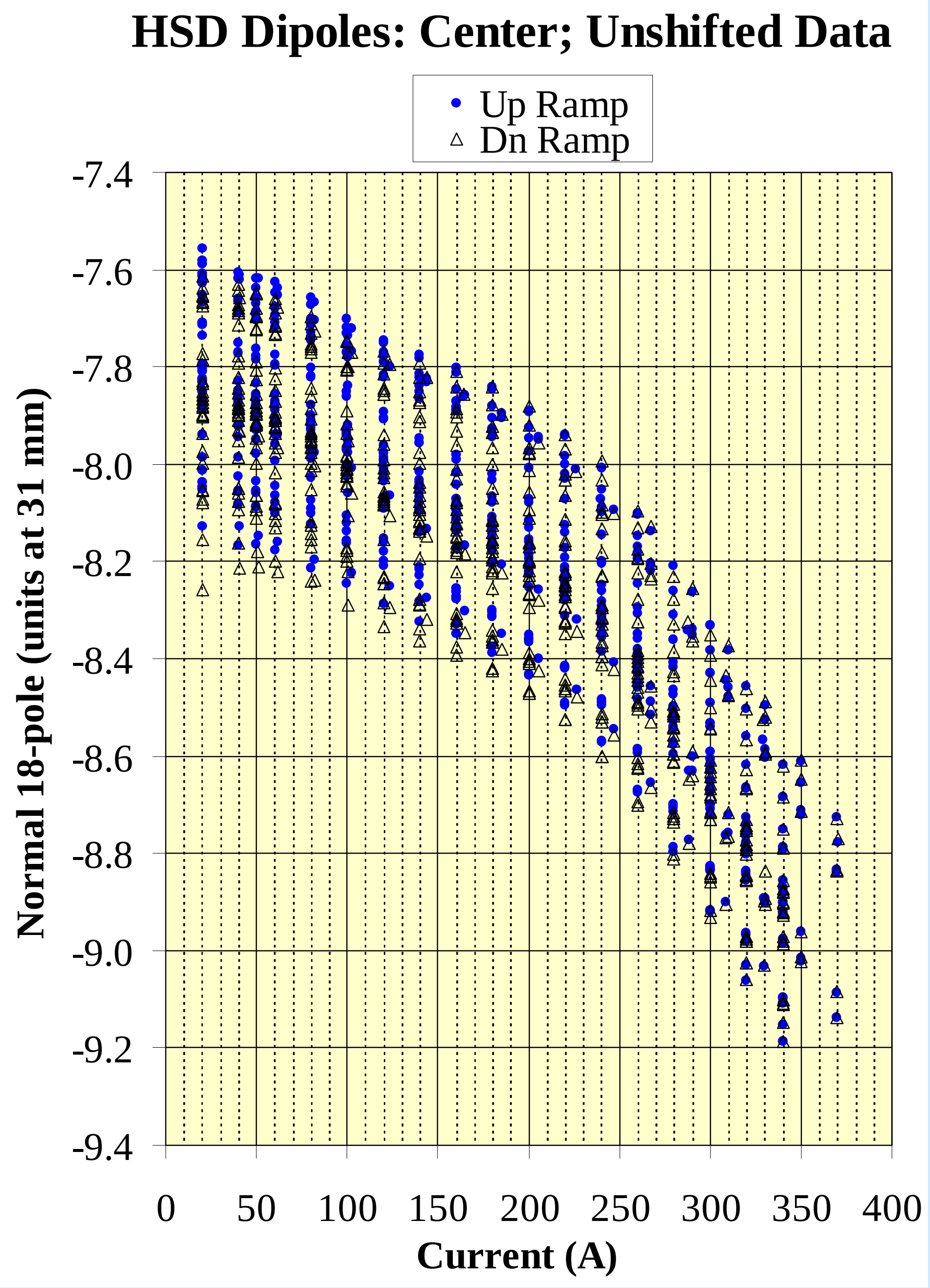
HSD Dipoles: Center; Unshifted Data
Up Ramp
Dn Ramp
Normal 18-pole (units at 31 mm)
-7.4
-7.6
-7.8
-8.0
-8.2
-8.4
-8.6
-8.8
-9.0
-9.2
-9.4
0
50
100
150
200
250
300
350
400
Current (A)

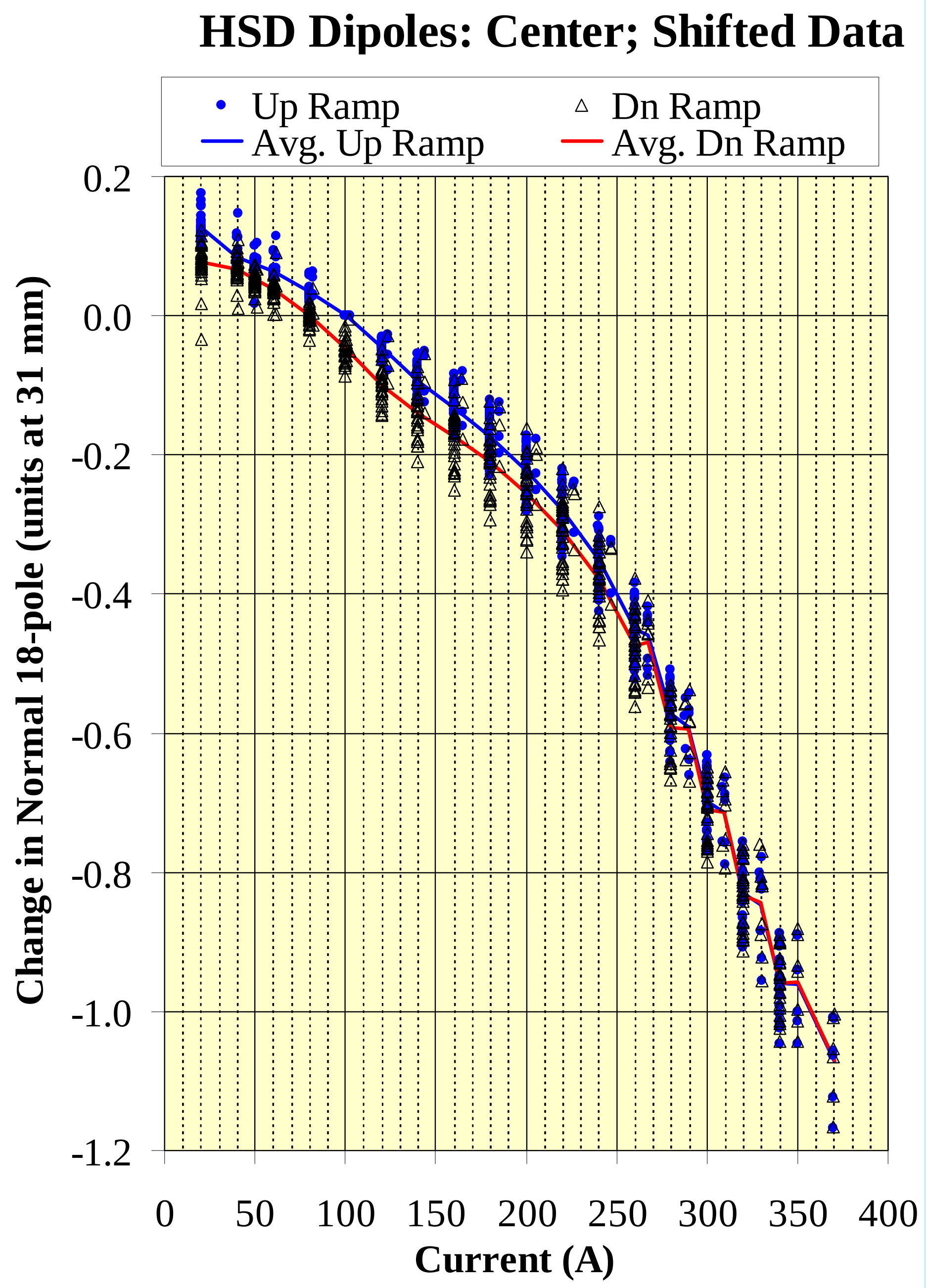
HSD Dipoles: Center; Shifted Data
Up Ramp
Dn Ramp
Avg. Up Ramp
Avg. Dn Ramp
Change in Normal 18-pole (units at 31 mm)
0.2
0.0
-0.2
-0.4
-0.6
-0.8
-1.0
-1.2
0
50
100
150
200
250
300
350
400
Current (A)

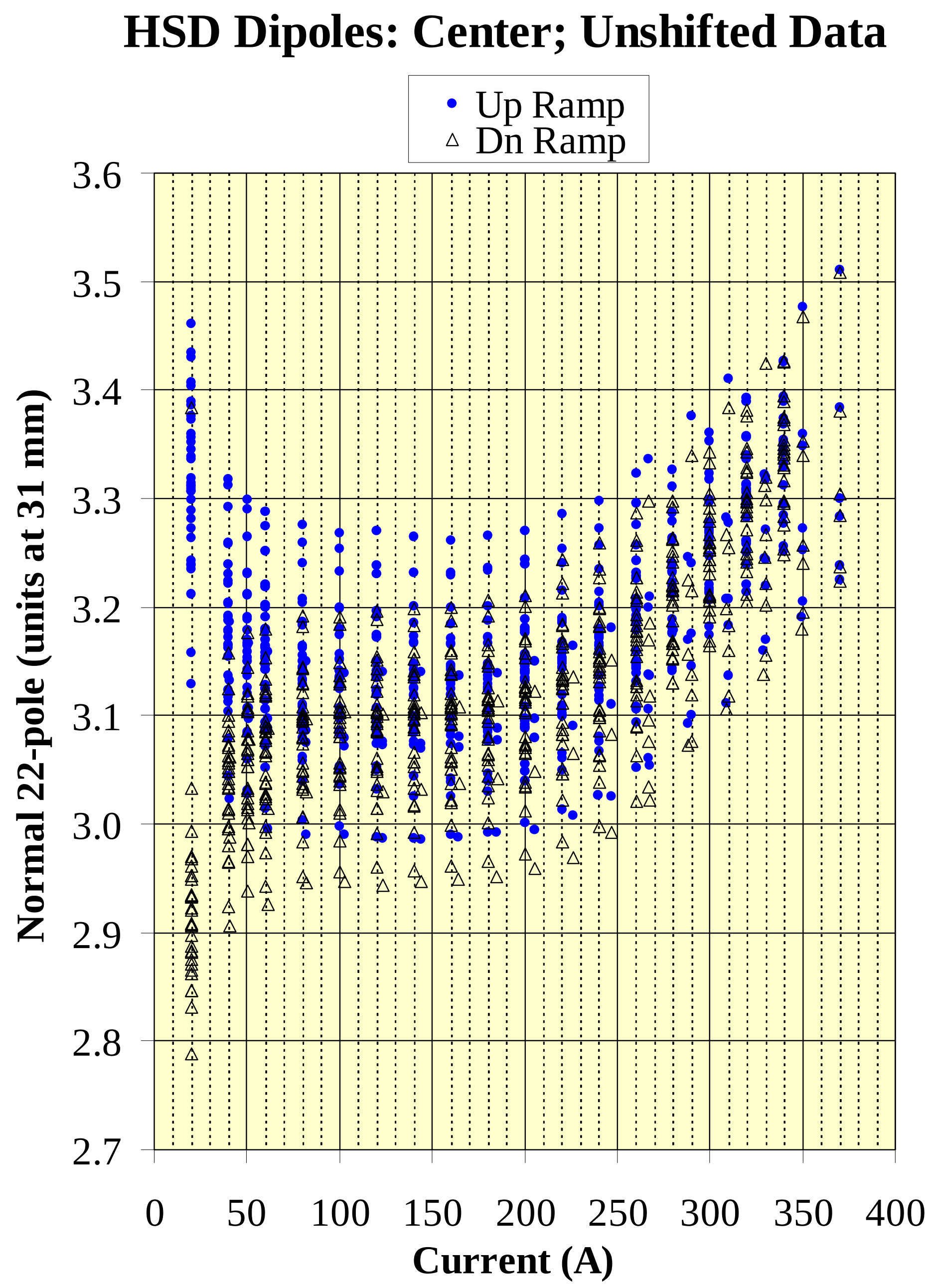
HSD Dipoles: Center; Unshifted Data
Up Ramp
Dn Ramp
Normal 22-pole (units at 31 mm)
3.6
3.5
3.4
3.3
3.2
3.1
3.0
2.9
2.8
2.7
0
50
100
150
200
250
300
350
400
Current (A)

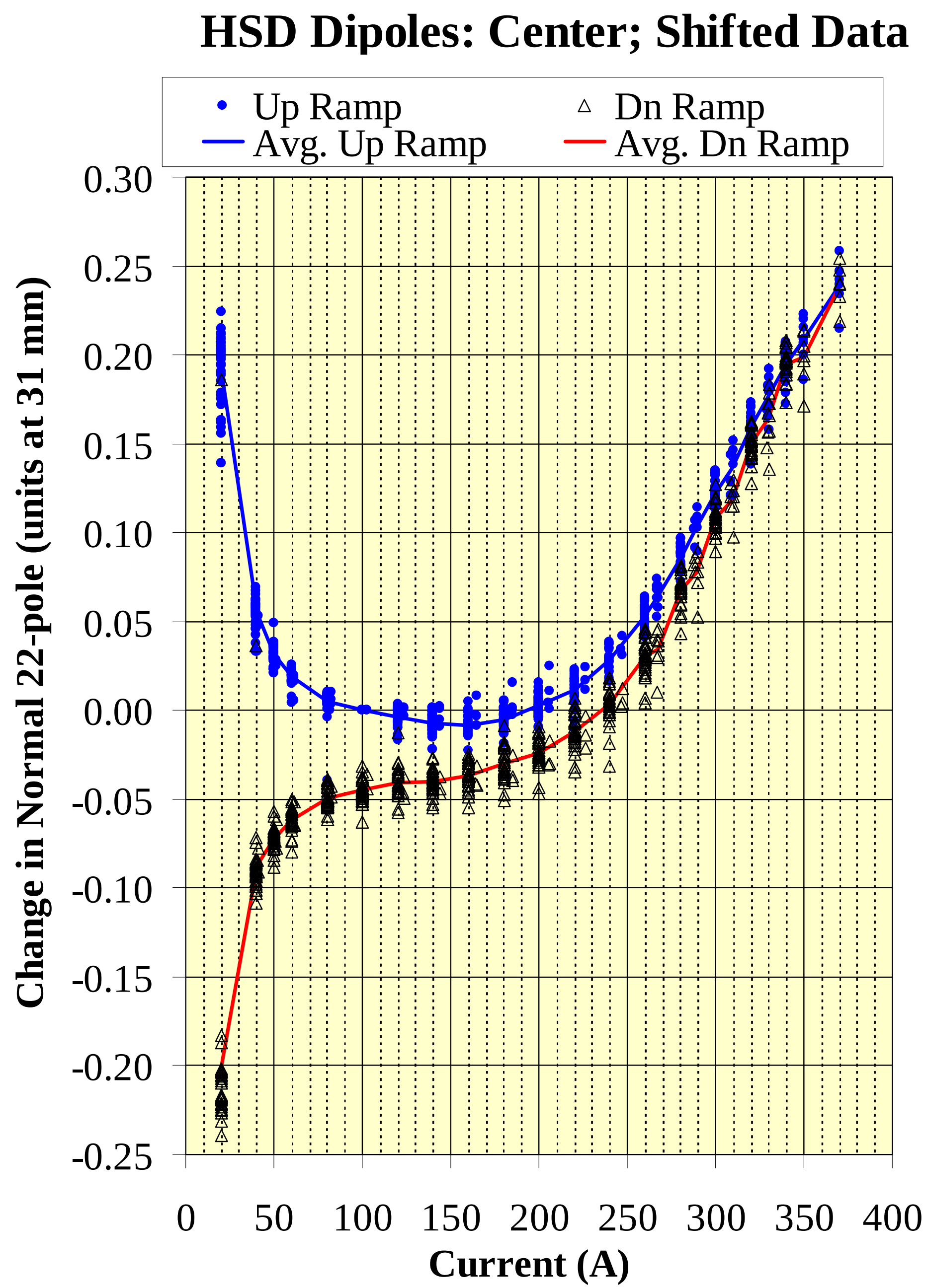
HSD Dipoles: Center; Shifted Data
Up Ramp
Dn Ramp
Avg. Up Ramp
Avg. Dn Ramp
Change in Normal 22-pole (units at 31 mm)
0.30
0.25
0.20
0.15
0.10
0.05
0.00
-0.05
-0.10
-0.15
-0.20
-0.25
0
50
100
150
200
250
300
350
400
Current (A)

Z-Scan Data

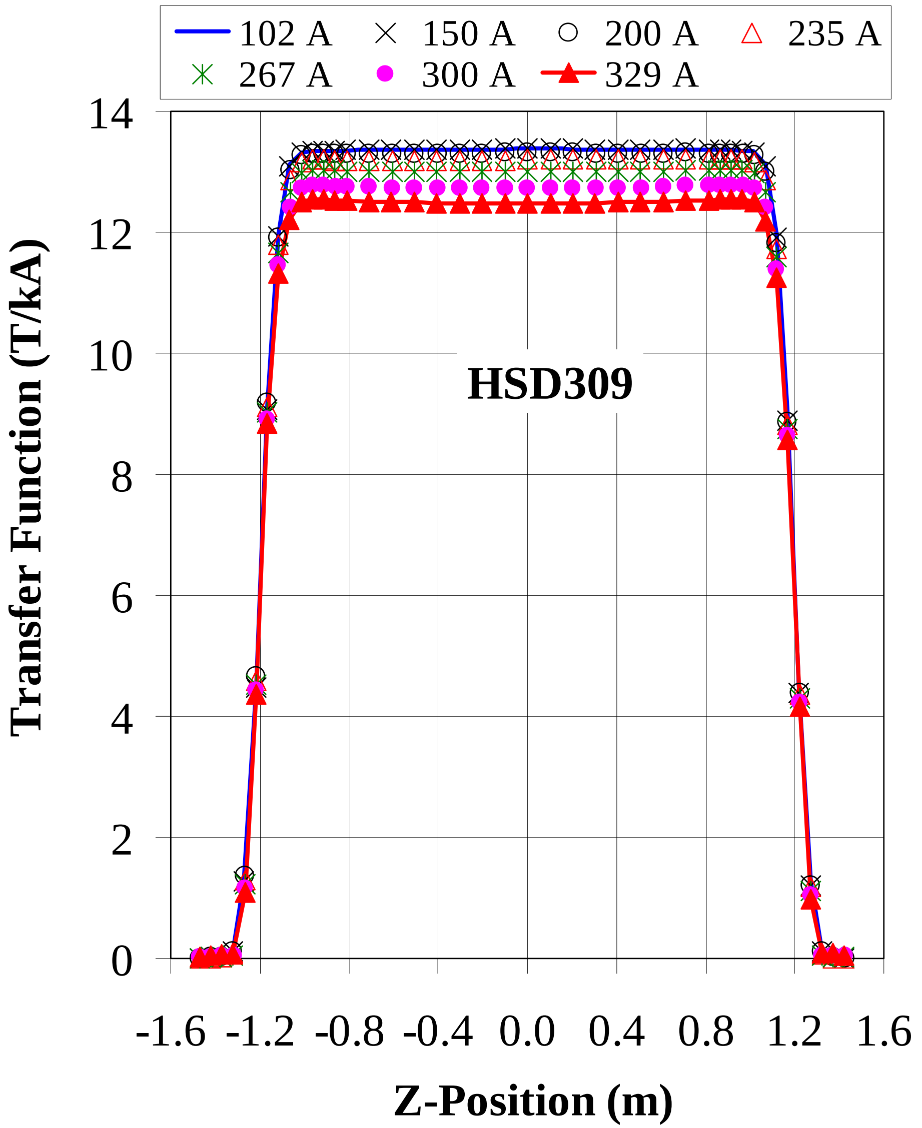

102 A
150 A
200 A
235 A
267 A
300 A
329 A
HSD309
Transfer Function (T/kA)
Z-Position (m)
0
2
4
6
8
10
12
14
-1.6 -1.2 -0.8 -0.4 0.0 0.4 0.8 1.2 1.6

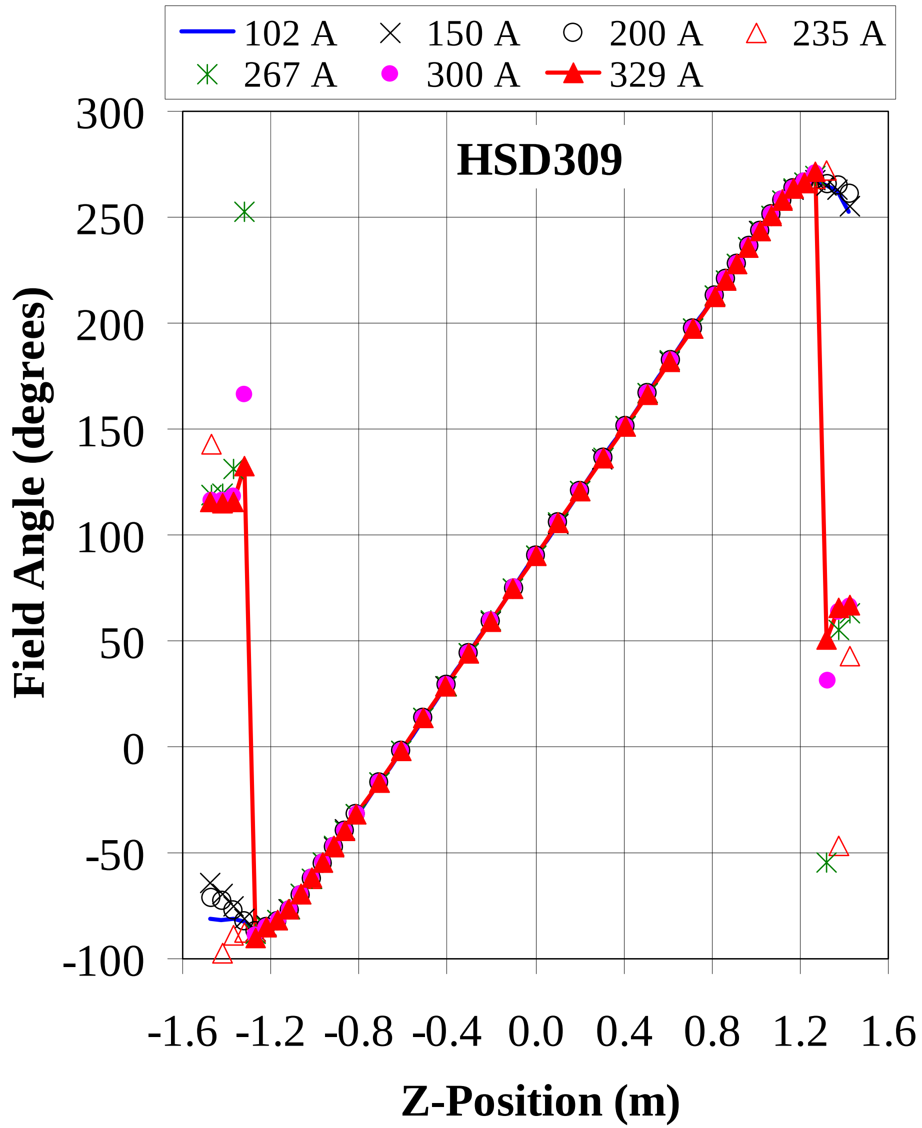

102 A
150 A
200 A
235 A
267 A
300 A
329 A
HSD309
Field Angle (degrees)
Z-Position (m)
-100
-50
0
50
100
150
200
250
300
-1.6 -1.2 -0.8 -0.4 0.0 0.4 0.8 1.2 1.6

Z-Scan Data

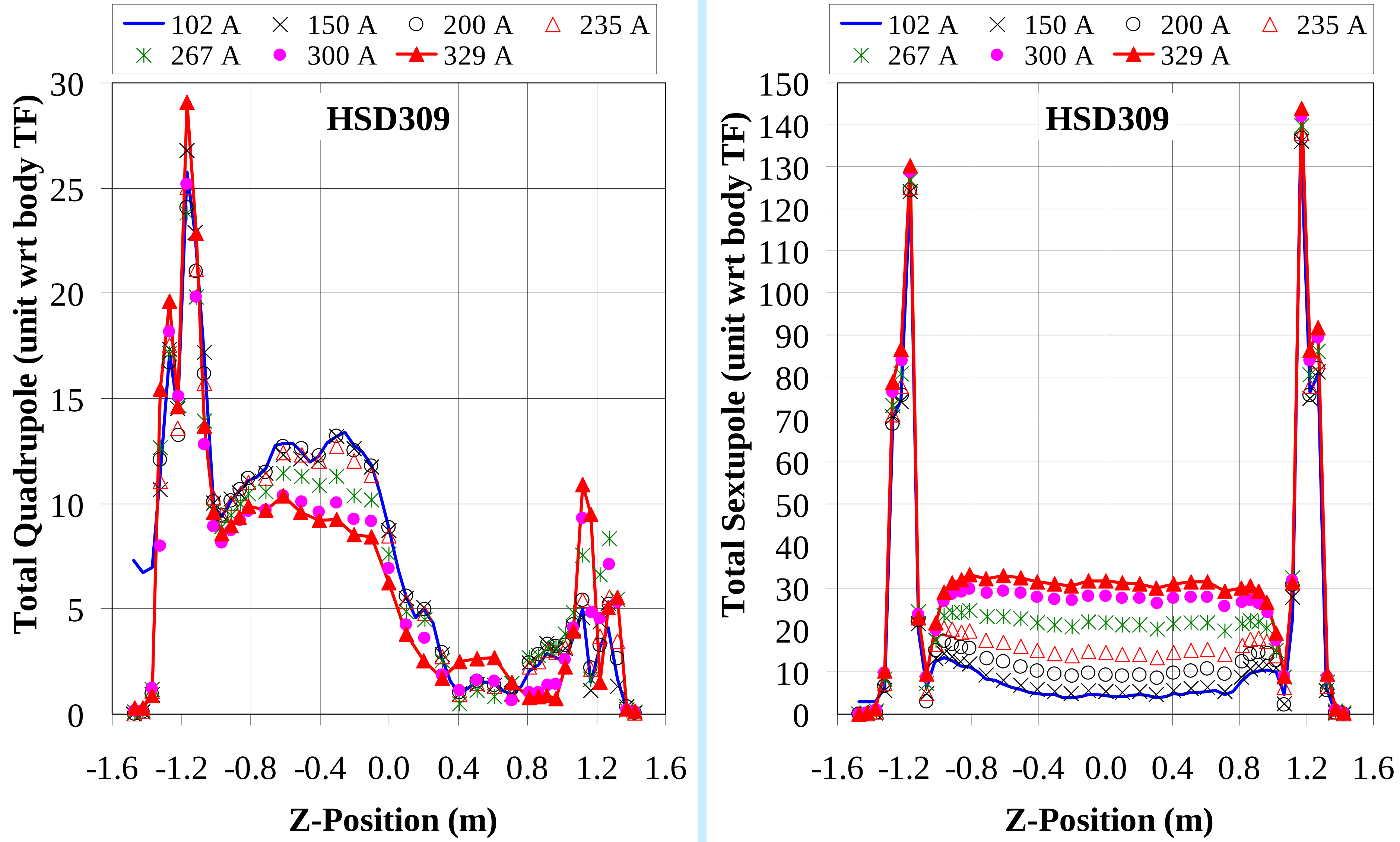

102 A
150 A
200 A
235 A
267 A
300 A
329 A
HSD309
Total Quadrupole (unit wrt body TF)
Z-Position (m)
HSD309
Total Sextupole (unit wrt body TF)
Z-Position (m)

Z-Scan Data

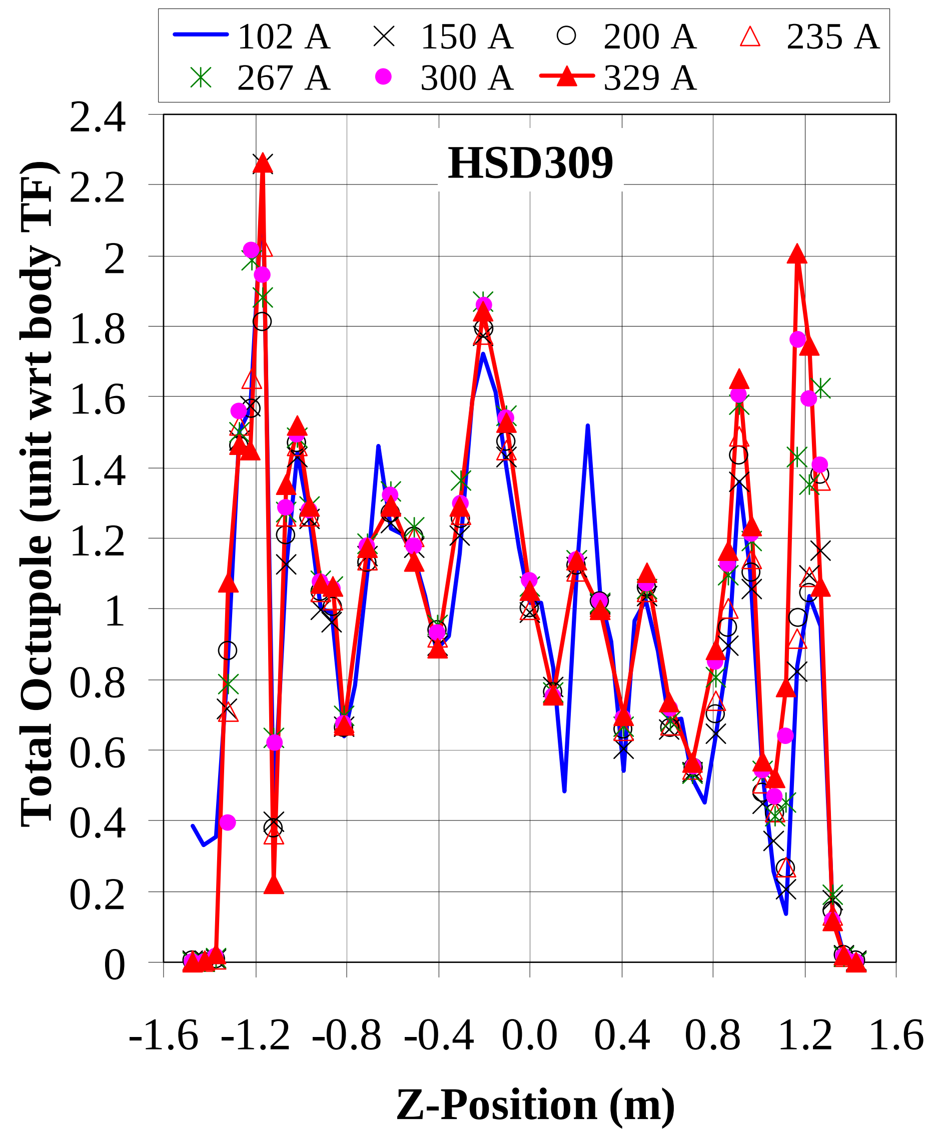

102 A
150 A
200 A
235 A
267 A
300 A
329 A
HSD309
Total Octupole (unit wrt body TF)
Z-Position (m)
2.4
2.2
2
1.8
1.6
1.4
1.2
1
0.8
0.6
0.4
0.2
0
-1.6
-1.2
-0.8
-0.4
0.0
0.4
0.8
1.2
1.6

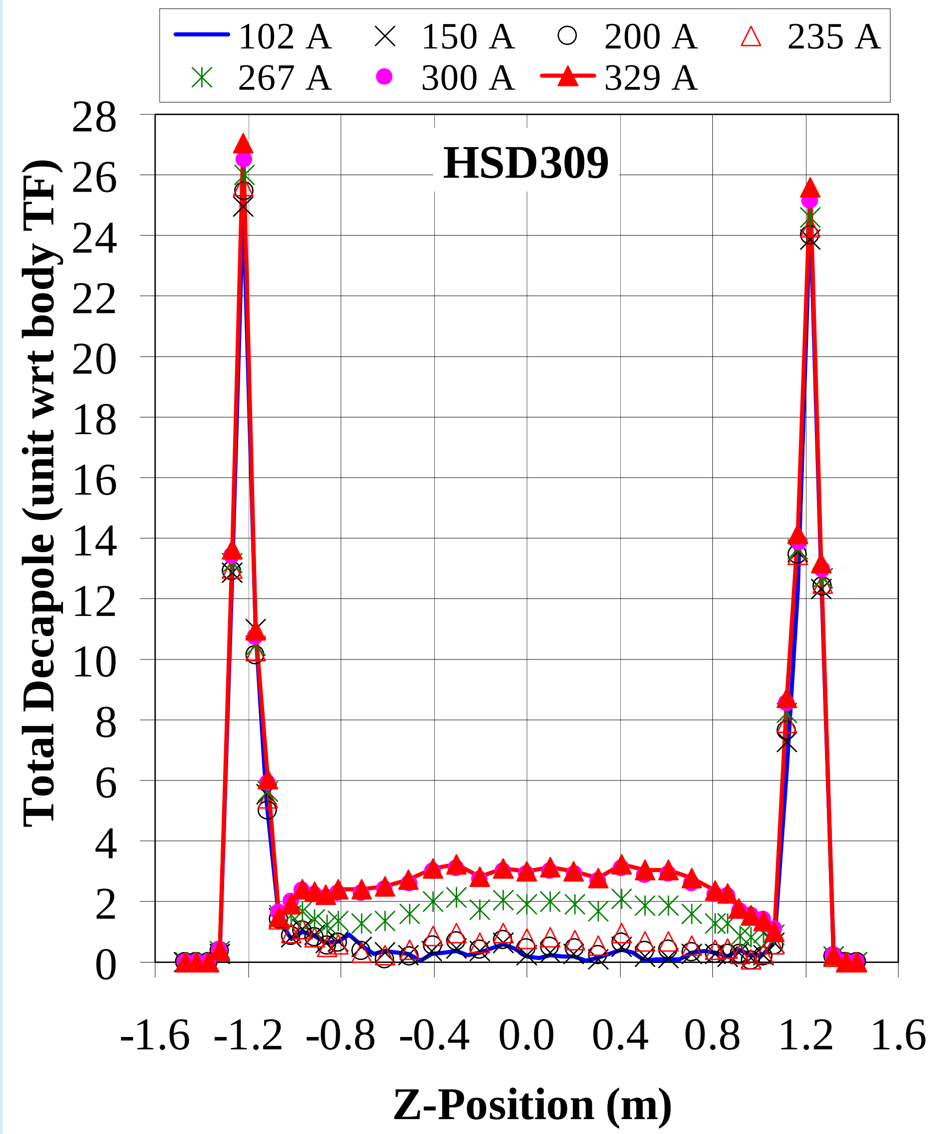

102 A
150 A
200 A
235 A
267 A
300 A
329 A
HSD309
Total Decapole (unit wrt body TF)
Z-Position (m)
28
26
24
22
20
18
16
14
12
10
8
6
4
2
0
-1.6
-1.2
-0.8
-0.4
0.0
0.4
0.8
1.2
1.6

Z-Scan Data

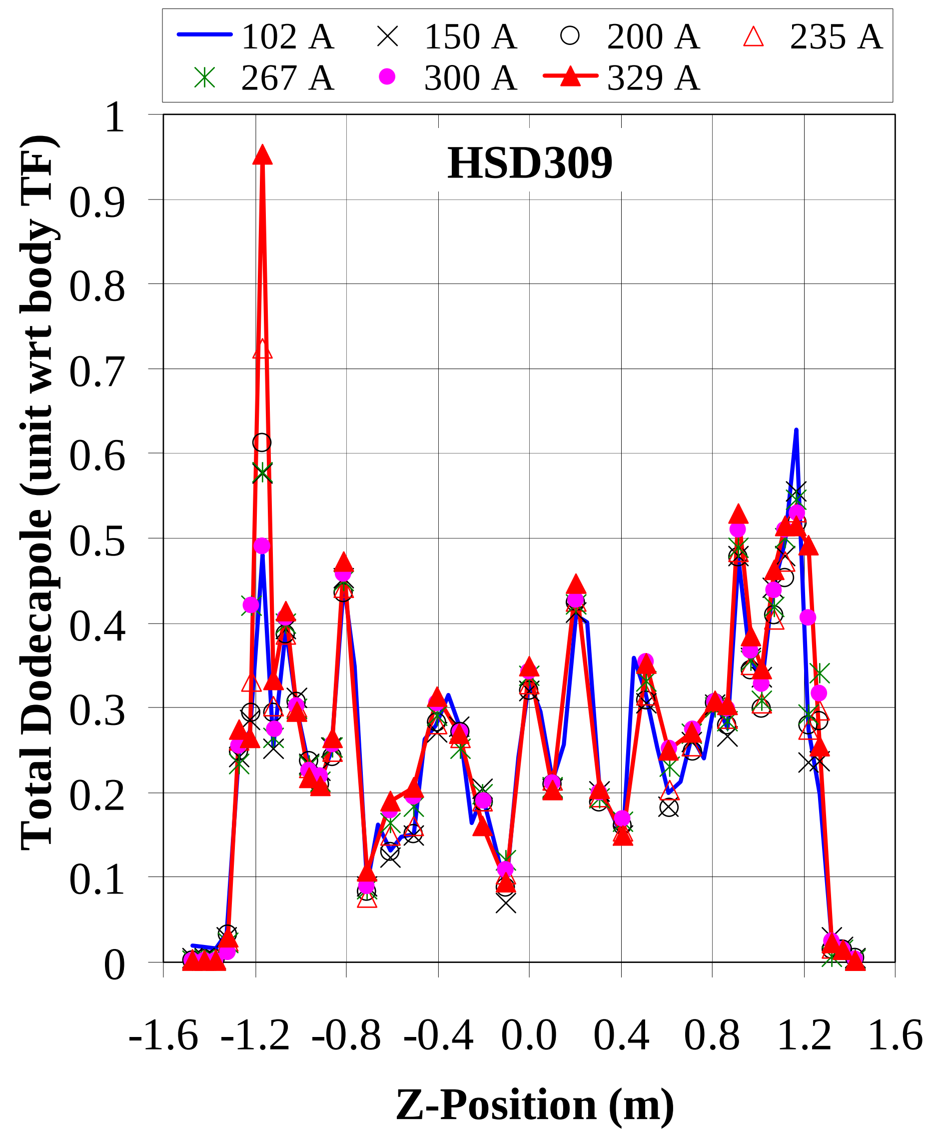

102 A
150 A
200 A
235 A
267 A
300 A
329 A
HSD309
Total Dodecapole (unit wrt body TF)
Z-Position (m)

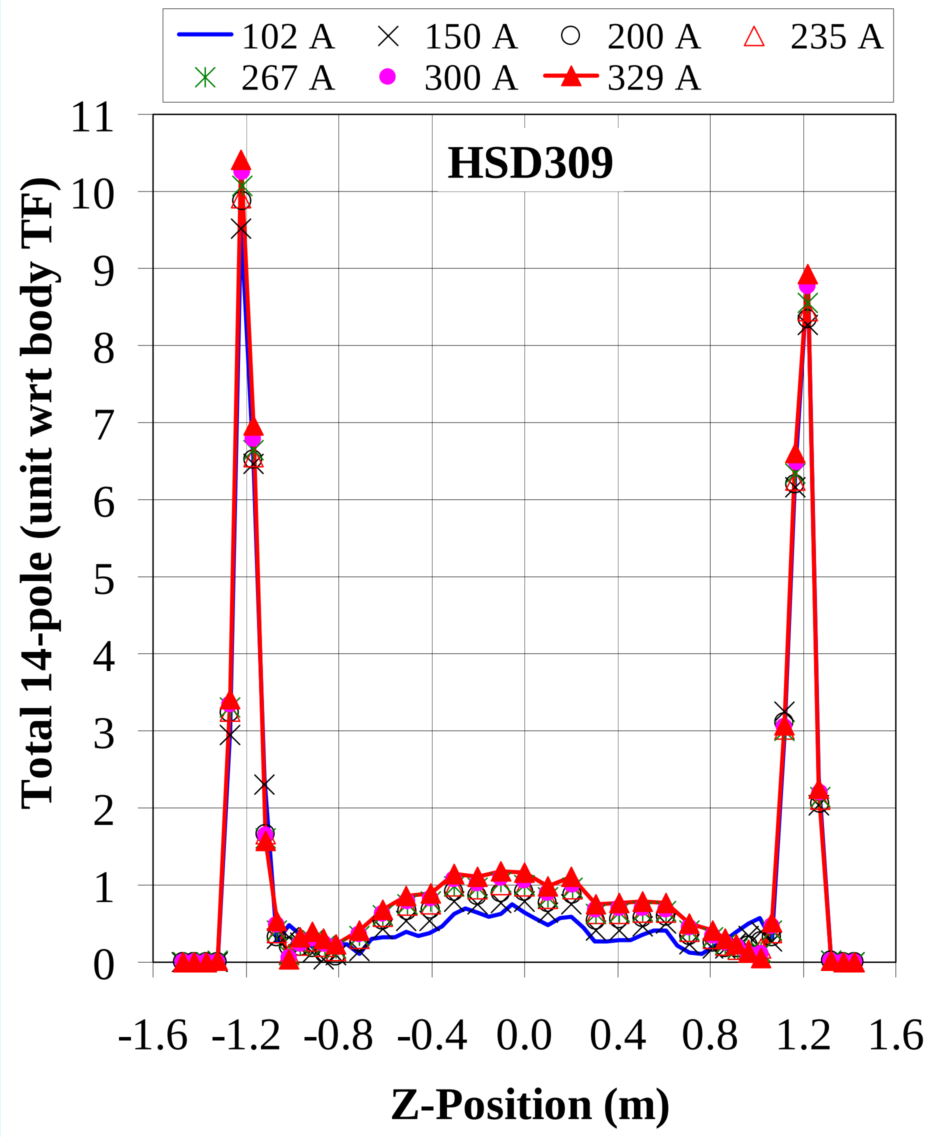

102 A
150 A
200 A
235 A
267 A
300 A
329 A
HSD309
Total 14-pole (unit wrt body TF)
Z-Position (m)

Z-Scan Data

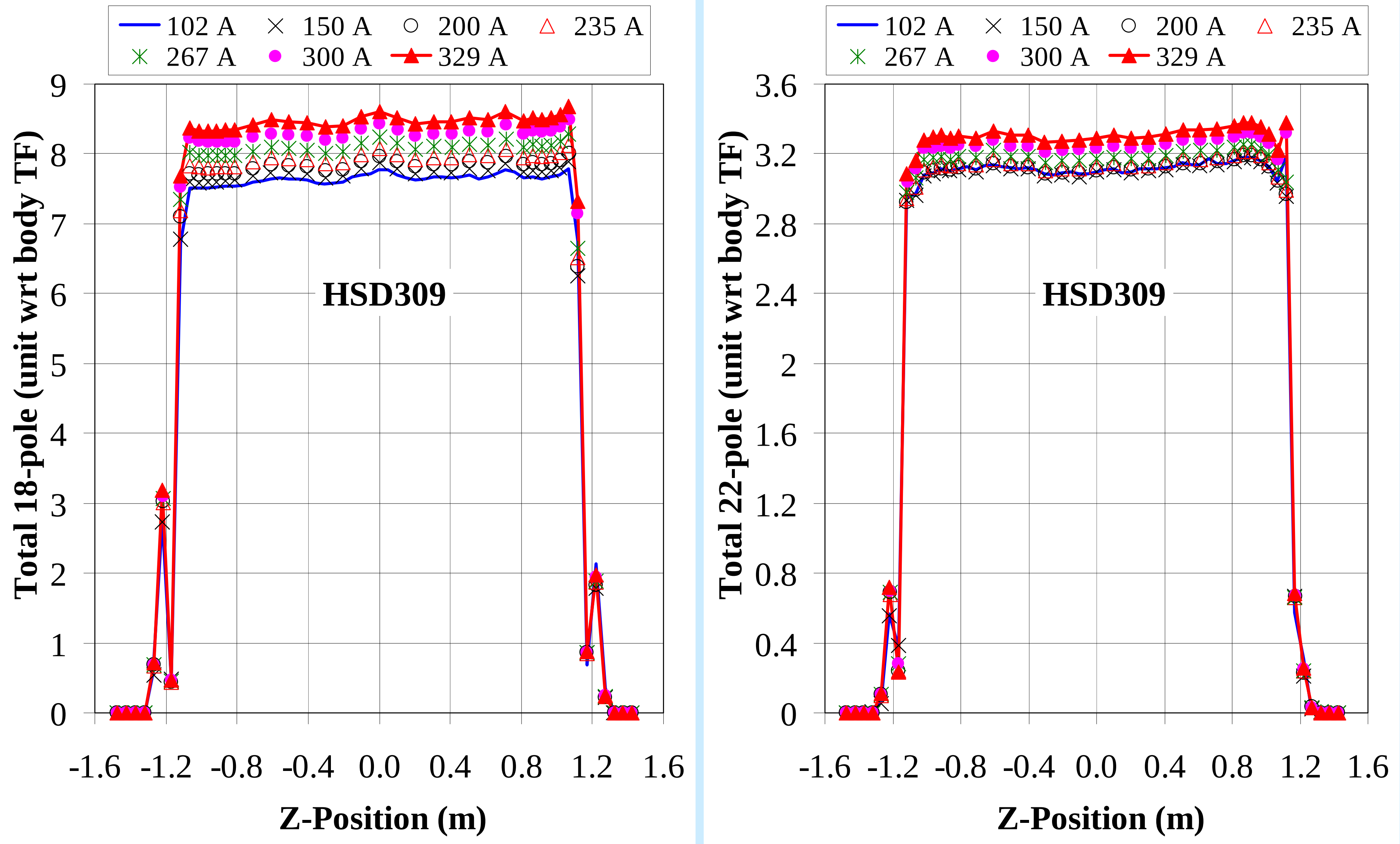
102 A
150 A
200 A
235 A
267 A
300 A
329 A
HSD309
Total 18-pole (unit wrt body TF)
9
8
7
6
5
4
3
2
1
0
-1.6
-1.2
-0.8
-0.4
0.0
0.4
0.8
1.2
1.6
Z-Position (m)
102 A
150 A
200 A
235 A
267 A
300 A
329 A
HSD309
Total 22-pole (unit wrt body TF)
3.6
3.2
2.8
2.4
2
1.6
1.2
0.8
0.4
0
-1.6
-1.2
-0.8
-0.4
0.0
0.4
0.8
1.2
1.6
Z-Position (m)

Conclusions

- A measuring coil system for use in helical dipoles is presented.
- The short length of the coil (51 mm) allows precise measurements of the higher order terms by avoiding any significant cancellation of harmonics.
- Current dependence of harmonics is shown to have small magnet to magnet variations.
- Z-scans in small axial increments shows significant axial variation in the lower order harmonics.
- Analysis of the end regions has scope for further improvements.